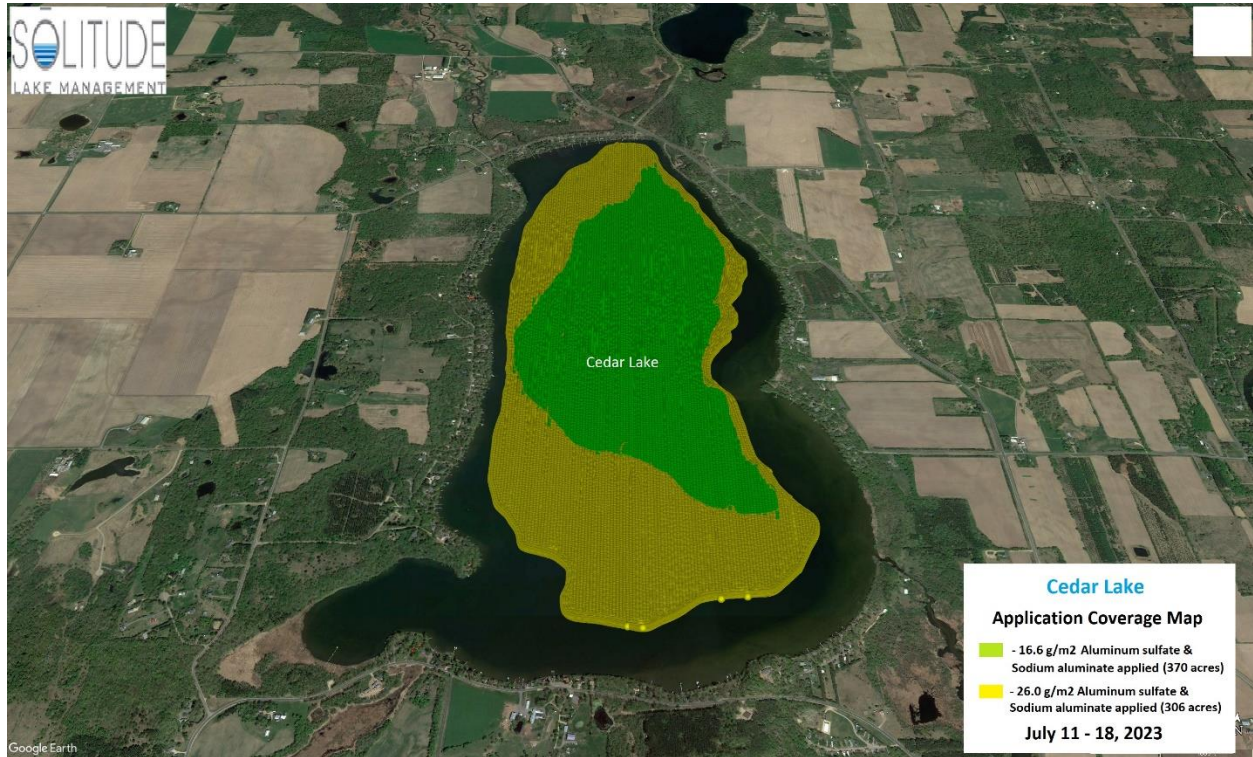# Cedar Lake, Wisconsin - Limnological response to alum treatment: 2023 interim report

Aerial map of alum application to Cedar Lake in 2023. Credits: Solitude Lake Management

16 February 2024

University of Wisconsin – Stout
Center for Limnological Research and Rehabilitation
Department of Biology
260 Jarvis Hall
Menomonie, Wisconsin 54751
715-338-4395
jamesw@uwstout.edu

Executive Summary

A comparison of mean summer (July-early October) summer concentrations of surface and bottom total phosphorus (P) and soluble reactive P (SRP), chlorophyll and Secchi transparency during a pretreatment year (2010) and the post-treatment years 2017-23.

- The 4th partial alum application occurred in mid-July 2023. Approximately 26 g Al/m^2 were applied to depth contours between 20 and 25 ft and 17 g Al/m^2 were applied to depths > 25 ft. In addition, buffered alum was used for the 4th application to reduce sulfate input and bacterial reduction in the sediment.

- The 2023 alum treatment was largely but not entirely successful in suppressing internal P loading. Alum application in mid-July was timed to occur shortly before anticipated turnover (which occurred in late August) to reduce soluble P entrainment and uptake by cyanobacteria. While hypolimnetic SRP accumulation was very minor throughout the summer, the concentration increased to ~ 0.085 mg/L by early September. Some of this P probably mixed into the surface waters during turnover, leading to a modest chlorophyll bloom that developed in September. However, soluble P entrainment appeared to be mostly suppressed compared to patterns in 2022.

- Bottom iron concentrations were ~ 0.5X lower in 2023 compared to 2010. This reduction is believed to be the result of formation of inert iron sulfide ($FeS_{(solid)}$) due to bacterial sulfate reduction to S and reaction with Fe^{2+} below the sediment-water interface. This removal process is significant because there is less "redox" Fe (i.e., dissolved Fe that diffuses into the water) to precipitate soluble P in the hypolimnion during turnover periods.

- These results suggest that for Cedar Lake, both complete anaerobic diffusive P flux suppression and balancing the Fe:P ratio so that it is > ~ 4:1 is needed to successfully control internal P loading. Specifically, anaerobic diffusive P flux still needs to be further reduced in both treatment zones to attain WQ goals. In addition, hypolimnetic Fe
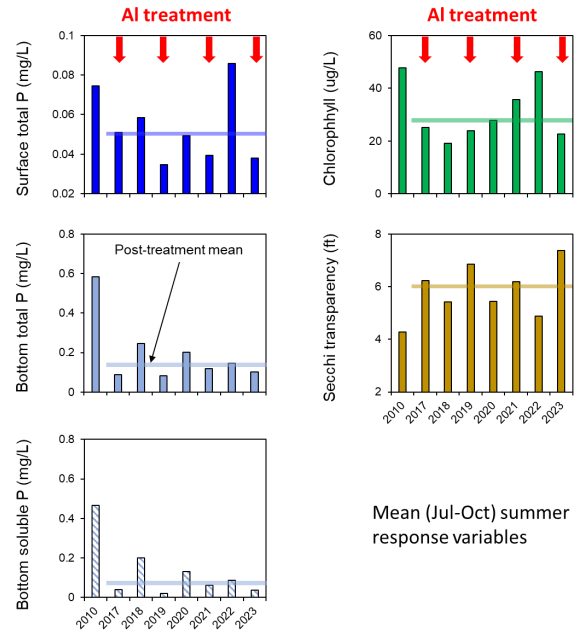
concentrations need to increase relative to hypolimnetic P to maintain the Fe:P mass ratio at >4:1.

- Mean bottom total P and SRP concentrations (JUL-OCT) were relatively low in 2023 at 0.102 mg/L and 0.038 mg/L, representing an 83% and 92% reduction, respectively, compared to 2010. Mean summer surface total P declined to 0.038 mg/L (49% decrease versus 2010). Unlike 2022 patterns, mean chlorophyll declined to 23 μg/L in 2023, 53% lower than the pretreatment average. Finally, mean Secchi transparency was improved in 2023 at 7.4 ft.

Objectives

Multiple Al applications over a period of 10-12 years are planned for Cedar Lake to control internal phosphorus loading. It is critical to conduct post-treatment monitoring of water and sediment chemistry to document the trajectory of water quality improvement during rehabilitation to make informed decisions regarding adjusting management to meet future water quality goals. Post-treatment monitoring included field and laboratory research to document changes in 1) hydrology and watershed phosphorus (P) loading, 2) the P budget and lake water quality, 3) binding of sediment mobile P fractions that have contributed to internal P loading by alum, and 4) rates of diffusive P flux from the sediment under anaerobic conditions. Overall, lake water quality was predicted to respond to watershed and internal P loading reduction with lower surface concentrations of total P and chlorophyll concentrations throughout the summer, lower bloom frequency of nuisance chlorophyll levels, and higher water transparency. Multiple Al applications between 2017 and 2025 should result in the binding of iron-bound P and substantial reduction in diffusive P flux from sediments under anaerobic conditions (i.e., internal P loading).

The first alum application occurred in late June 2017. The Al dose was 20 g/m^2 for sediment located within the 20-25 ft depth contour and 26 g/m^2 for sediment located at depths > 25 ft. The second alum application occurred during 11-22 June 2019 and Al concentrations ranged between 22 g/m^2 within the 20-25 ft depth contour and ~ 28 g/m^2 for depths > 25 ft. This combined Al application of 42 g/m^2 and 54 g/m^2 to the two depth zones ideally represented ~ 42% of the target Al doses of 100 g/m^2 and 130 g/m^2. However, sediment monitoring suggested the Al floc had spread and become diluted particularly at depths > 25 ft, resulting in lower measured Al

concentrations than predicted. Lower Al recovery might be attributed to Al floc movement or redistribution and spread during and after application by wind activity and water currents. Al floc movement during settling is not uncommon and has been reported to occur in other alum treatments (Egemose et al. 2009, 2013; Huser 2017; James and Bischoff 2020). As an adaptive management decision, the third alum treatment in June 2021 was applied to sediments located at depths > 25 ft only to increase the overall Al concentration and thickness of the Al floc in this deeper area of the lake. Since this area is smaller than the earlier combined application area encompassing depths > 20 ft (332 ac), the Al dosage was increased to ~ 50 g/m^2 within the > 25-ft zone without increasing overall costs.

The fourth alum application occurred in 2023. It was hypothesized that use of aluminum sulfate for the first 3 treatments led to interference with the iron cycle in the lake via iron sulfide formation as a result of bacterial reduction of sulfate to S by anaerobic bacteria at the sediment-water interface. Because P binding in the Al floc layer was still not complete due to partial dosage application, some sediment P has still been diffusing through the Al floc layer into the water column. P availability during fall turnover in 2022 led to a cyanobacteria bloom with chlorophyll concentrations exceeding 100 µg/L.

In 2023, application strategy was changed 4-fold to improve P binding efficiency. First, the product was switched to buffered alum to reduce sulfate input to the lake. Second, since no alum was applied to the 20-25-ft depth contour in 2021, a higher alum dose was applied to the 20-25-ft depth contour in 2023 to achieve dosage requirements in this area of the lake. Third, to meet budget constraints (since buffered alum is more expensive than aluminum sulfate), the buffered alum dose was reduced to 26 g Al/m^2 applied to the 20-25-ft depth contour and 16.6 g Al/m^2 applied to the > 25-ft depth contour. Finally, the alum application window was moved to mid-July, just before anticipated turnover, to strip any hypolimnetic P from the water column to minimize P uptake by cyanobacteria.

The objectives of this interim report were to describe the 2023 limnological and sediment variable response to these alum treatments in Cedar Lake. Limnological monitoring is being used in conjunction with an adaptive management approach to gauge lake response and the need, if

any, to adjust Al dose or application strategy.

Methods

Watershed loading and lake monitoring

A gauging station was established on Horse Creek above Cedar Lake at 10th Ave for concentration, loading, and flow determination between May and October 2023 (Fig. 1). Unfortunately, the flow velocity equipment was vandalized and destroyed in late July 2021. A water level pressure transducer (Onset, Inc) was deployed and maintained by Polk County soil and Water Conservation District in 2023. Discrete flow velocity measurements were collected at biweekly intervals between May and October 2023 using a Marsh-McBirney Flow-Mate 2000 velocity probe to develop a stage elevation-flow relationship for estimating continuous flow from the continuous stage elevation record. Grab samples were collected biweekly at the 10th Ave gauging station for chemical analysis. Additional samples were collected biweekly at a Horse Creek station on County Y, located below Horse Lake. Water samples were analyzed for total suspended solids (TSS), total volatile solids (VSS), total P, and soluble reactive P (SRP) using standard methods (APHA 2011). Summer tributary P loading was calculated using the computer program FLUX.

The deep basin water quality station WQ 2 was sampled biweekly between May and October 2023 (Fig. 1). An integrated sample over the upper 2-m was collected for analysis of total P, SRP, and chlorophyll a. Additional discrete samples were collected at 1-m intervals to within 0.5 m of the sediment surface for analysis of total P, SRP, and chlorophyll. Secchi transparency and in situ measurements (temperature, dissolved oxygen, pH, and conductivity) were collected on each date using a YSI 6600 sonde (Yellow Springs Instruments) that was calibrated against dissolved oxygen Winkler titrations (APHA 2011) and known buffer solutions.

Sediment chemistry

Sediment characteristics. A sediment core was collected in September 2023 at WQ 2 (Fig. 1) for

determination of vertical profiles of various sediment characteristics and phosphorus fractions (see Analytical methods below). The sediment core was sectioned at 1-cm intervals between 0 and 10 cm and at 2-cm intervals below the 10-cm depth for determination of moisture content, wet and dry bulk density, loss-on-ignition organic matter, loosely-bound P, iron-bound P, labile organic P, aluminum-bound P, and total aluminum. Additional cores were collected at stations 2, 8, 18, and 24 located along a transect that was established in 2012 (Fig. 1). An upper 10 cm slice was sectioned for the variables listed above..

Laboratory-derived diffusive phosphorus flux from sediments under anaerobic conditions.
Anaerobic diffusive P fluxes were measured from intact sediment cores collected at stations shown in Figure 1 in September 2023. Three sediment cores were collected at WQ 2 and one sediment core was collected at each spatial station to monitor alum treatment effectiveness after 2023 alum application. The sediment incubation systems were placed in a darkened environmental chamber and incubated at 20 C for up to 7 days. The incubation temperature was set to a standard temperature for all stations for comparative purposes. The oxidation-reduction environment in each system was controlled by gently bubbling nitrogen through an air stone placed just above the sediment surface to maintain anaerobic conditions.

Water samples for SRP were collected from the center of each system using an acid-washed syringe and filtered through a 0.45 µm membrane syringe filter (Nalge). The water volume removed from each system during sampling was replaced by addition of filtered lake water preadjusted to the proper oxidation-reduction condition. These volumes were accurately measured for determination of dilution effects. Rates of P release from the sediment (mg/m^2 d) were calculated as the linear change in mass in the overlying water divided by time (days) and the area (m^2) of the incubation core liner. Regression analysis was used to estimate rates over the linear portion of the data.

Analytical methods. A known volume of sediment was dried at 105 ^{o}C for determination of moisture content, wet and dry bulk density, and burned at 550 ^{o}C for determination of loss-on-ignition organic matter content (Avnimelech et al. 2001, Håkanson and Jansson 2002). Phosphorus fractionation was conducted according to Hieltjes and Lijklema (1980), Psenner and

Puckso (1988), and Nürnberg (1988) for the determination of ammonium-chloride-extractable P (loosely-bound P), bicarbonate-dithionite-extractable P (i.e., iron-bound P), and sodium hydroxide-extractable P (i.e., aluminum-bound P).

The loosely-bound and iron-bound P fractions are readily mobilized at the sediment-water interface as a result of anaerobic conditions that lead to desorption of P from sediment and diffusion into the overlying water column (Mortimer 1971, Boström 1984, Nürnberg 1988). The sum of the loosely-bound and iron-bound P fraction represents redox-sensitive P (i.e., the P fraction that is active in P release under anaerobic and reducing conditions) and will be referred to as **redox-P**. Aluminum-bound P reflects P bound to the Al floc after aluminum sulfate application and its chemical transformation to aluminum hydroxide ($Al(OH)_3$).

Summary of Results

Hydrology and phosphorus loading

On an annual basis, precipitation in 2023 was near the~ 33-inch average since 1980 at ~30 inches (Fig. 2). Monthly precipitation at Amery in 2023 was well below the long-term average in May, June, and August, and near average in July and September (Fig. 3). Unfortunately, the stage logger at 10th Ave malfunctioned between July and September (Fig. 4). Daily precipitation was relatively low during this period and below average. However, the logger apparently did not detect increases in stage during some storms in mid-June through August. During that period, daily precipitation at Amery exhibited peaks of 0.89 on 25 June, 1.06 on 3 July, 0.75 on 23 July, a total of 1.54 between 26-28 July, and 0.84 on 14 August. Thus, summer mean daily flow at 10th Ave was underestimated in 2023 (Fig. 5).

Similar to other years, total P concentrations in Horse Creek at 10th Ave were higher during the Spring period of May through early June precipitation, ranging between 0.055 mg/L and 0.096 mg/L (Fig. 6). Concentrations declined to 0.043 – 0.057 mg/L during the lower flow period of mid-July through August, then increased during storm-generated inflows in late September. Soluble reactive P concentrations were relatively constant during the study period at ~ 0.021

mg/L. TSS and VSS concentrations were highest in late May at ~23 mg/L and 13 mg/L, respectively, and declined to nominal levels between June and August. Concentration increased in October in conjunction with precipitation events on 14 October (1.21 in) and 26 October (0.72 in).

Total P concentrations at Horse Creek at County Y, located below Horse Lake, fluctuated between 0.053 mg/L and 0.121 mg/L. SRP concentrations were low to undetectable in the discharge of Horse Lake. Unlike the relatively lower concentrations at 10th Ave, TSS and VSS were higher in concentration at County Y during the summer. Summer variable concentration differences between the two stations suggested, 1) TSS-VSS concentration peaks at 10th Ave in May probably originated from watershed sources located between Horse Lake and Cedar Lake and this load likely entered Cedar Lake, 2) high TSS-VSS and total P concentrations originating from Horse Lake after July probably settled in the Horse Creek floodplain upstream of Cedar Lake (i.e., County Y TSS-VSS and total P >> 10th Ave TSS-VSS and total P), and 3) SRP loads probably originated downstream of Horse Lake during the summer (i.e., County Y SRP << 10th Ave SRP). Similar upstream-downstream patterns were observed during the 2009-2011 monitoring period (James 2014).

Concentration-flow relationships in 2023 were shifted compared to historical patterns (Fig. 7). This anomaly was likely related to stage logger failure in 2023. Flow-averaged summer total P in 2023 was slightly lower at 0.066 mg/L compared to other years (Table 1 and Fig. 7). The flow-averaged SRP concentration was 0.021 mg/L and accounted for ~ 32% of the total P in 2023. Summer loading could not be determined in 2023 due to stage logger failure.

Table 1. Mean summer (May-October) constituent concentrations and loading for the Horse Creek inflow station at 10th Ave. Summer loading could not be determined in 2023 due to logger failures during the summer.

Year	Variable	TSS	Total P	SRP
2010	Concentration (mg/L)		0.089	0.031
	Load (kg/d)		4.18	1.42
2017	Concentration (mg/L)	15.2	0.084	0.034
	Load (kg/d)	767.8	4.26	1.71
2018	Concentration (mg/L)	16.5	0.100	0.039
	Load (kg/d)	549	3.36	1.28
2019	Concentration (mg/L)	10.6	0.083	0.035
	Load (kg/d)	524	4.07	1.72
2020	Concentration (mg/L)		0.083	0.033
	Load (kg/d)		6.14	2.35
2021	Concentration (mg/L)[1]	22.1	0.082	0.021
	Load (kg/d)[2]	945	3.49	0.88
2022	Concentration (mg/L)	13.9	0.070	0.023
	Load (kg/d)	584	2.93	0.97
2023	Concentration (mg/L)	8.65	0.066	0.021
	Load (kg/d)	Not determined - Logger failure		
		Flow logger vandalized		

[1]Represents a flow-weighted mean between APR-JUL only
[2]Represents an estimated daily load between APR-JUL only

Lake limnological response

Stratification developed in mid-May and persisted until late August (Fig. 8). Hypolimnetic anoxia also developed in conjunction with stratification in mid-May and persisted until the late August turnover. Bottom anoxia was usually confined depths ≥ 7 m but extended to below the ~ 6-m depth in late June. The lake completely mixed in early September, resulting in reoxygenation of the entire water column. Isothermal and oxygenated conditions continued through mid-October.

Immediately prior to the start of alum application in mid-July, bottom total P and SRP concentrations were elevated at 0.090 mg/L TP and 0.057 mg/L SRP (Fig. 9 and 10). The 2023 alum application resulted in initial suppression of bottom P concentrations throughout July and early August. Bottom total P and SRP increased slightly to a peak 0.210 mg/L and 0.085 mg/L respectively in early September. Unlike patterns in 2022, turnover was associated with a decline in both total P and, in particular, SRP. This pattern may have been related to low hypolimnetic SRP relative to dissolved iron during turnover, as discussed later.

Surface total P concentrations were relatively low (≤ 0.020 mg/L) prior to alum treatment and declined further to ≤ 0.015 mg/L during the alum application in late July (Fig. 10 and 11). Total P concentration increased between mid-August and September, reflecting the development of a modest algal bloom. However, surface SRP remained undetectable (not shown) during turnover in late August, which differed from patterns of high SRP concentration during turnover in 2022.

Prior to alum treatment in mid-July, chlorophyll concentrations were relatively low, exhibiting a peak of only 16 µg/L on 27 June (Fig. 10 and 12, Appendix I). During the July alum application, chlorophyll declined to < 10 µg/L. However, by mid-August, a modest bloom developed that extended into September. The bloom concentration peak was 48 µg/L in late September. Chlorophyll increases reflected similar increases in surface total P, suggesting P uptake by algal for growth. Overall, total P and chlorophyll were significantly related, indicating P limitation of algal growth (Fig. 14).

Secchi transparency exceeded 5 m (17 ft) in May and declined to ~ 2.5 m in late June-early July,

reflecting the very modest chlorophyll concentration increases during the same period (Fig. 13). Secchi transparency increased substantially during the mid-July alum application period. It then declined as a result of the modest algal bloom that developed during mid-August through September. Secchi transparency exhibited a significant inverse pattern to that of chlorophyll, indicating that light extinction was due to algae versus inorganic turbidity (Fig. 14).

A comparison of mean summer (July-early October) limnological response variables before alum treatment (i.e., 2010) versus 2023 is shown in Figure 15 and Table 2. Mean bottom total P and SRP concentrations were relatively low in 2023 (Fig. 15), representing an 83% and 92% reduction, respectively, compared to 2010 (Table 2). Mean summer surface total P declined to 0.038 mg/L (49% decrease versus 2010, Table 2). Unlike 2022 patterns, mean chlorophyll declined to 23 µg/L in 2023, 53% lower than the pretreatment average. Finally, mean Secchi transparency was improved in 2023 at 7.4 ft (Fig. 15 and Table 2).

Table 2. Summary of changes in lake water quality and sediment variables after the initial alum treatment in June 2017. Overall goals after completion of the treatment schedule are shown in the last column.

		Variable	2010	2017	2018	2019	2020	2021	2022	2023	Percent improvement over 2010 means							Goal after internal P loading
											2017	2018	2019	2020	2021	2022	2023	
Lake	Mean (Jul-Oct)	Mean surface TP (mg/L)	0.074	0.051	0.058	0.035	0.050	0.040	0.086	0.038	31% reduction	22% reduction	53% reduction	34% reduction	47% reduction	15% increase	49% reduction	< 0.040
		Mean bottom TP (mg/L)	0.583	0.088	0.246	0.082	0.203	0.120	0.148	0.102	85% reduction	58% reduction	86% reduction	65% reduction	79% reduction	75% reduction	83% reduction	< 0.050
		Mean bottom SRP (mg/L)	0.467	0.038	0.199	0.02	0.130	0.062	0.086	0.038	92% reduction	57% reduction	96% reduction	72% reduction	87% reduction	82% reduction	92% reduction	< 0.050
		Mean chlorophyll (ug/L)	47.63	25.17	19.08	24.31	27.88	35.66	46.31	22.57	47% reduction	60% reduction	49% reduction	41% reduction	25% reduction	3% reduction	53% reduction	< 15
		Mean Secchi transparency (ft)	4.27	6.28	5.41	6.81	5.43	6.19	4.88	7.38	46% increase	27% increase	59% increase	27% increase	45% increase	14% increase	73% increase	12.1
	Early Fall peak (i.e. late August-early October)	Surface TP (mg/L)	0.130	0.081	0.115	0.042	0.074	0.060	0.136	0.061	38% reduction	11% reduction	68% reduction	43% reduction	54% reduction	5% increase	53% reduction	NA
		Bottom TP (mg/L)	1.216	0.13	0.543	0.206	0.510	0.223	0.227	0.210	89% reduction	55% reduction	83% reduction	58% reduction	82% reduction	81% reduction	83% reduction	NA
		Bottom SRP (mg/L)	1.092	0.068	0.468	0.092	0.442	0.156	0.193	0.085	94% reduction	57% reduction	92% redcuion	60% redcution	86% reduction	82% reduction	92% reduction	NA
		Chlorophyll (ug/L)	109.6	42.95	27.63	42.00	64.89	69.70	106.50	48.02	61% reduction	75% reduction	62% reduction	41% reduction	36% reduction	3% reduction	56% reduction	NA
		Secchi transparency (ft)	2.66	3.61	3.63	3.94	3.12	3.61	2.63	3.60	36% increase	37% increase	48% increase	17% increase	36% increase	1% reduction	35% increase	NA
Sediment[1]		Net internal P loading (kg/summer)	3,723	1,150	2,123	-177	1,351	404	3,103	955	69% reduction	42% reduction	100% reduction	64% reduction	89% reduction	17% reduction	74% reduction	< 400
		Net internal P loading (mg/m² d)	8.8	3.2	5.6	-0.5	2.8	1.1	8.5	3.9	64% reduction	36% reduction	100% reduction	68% reduction	88% reduction	3% reduction	56% reduction	< 1.5
		Sediment diffusive P flux (mg/m² d)	15.01	11.83	8.34	1.26	4.66	3.72	3.68	6.5	21% reduction	29% reduction	85% reduction	69% reduction	75% reduction	75% reduction	57% reduction	< 1.5
		Redox-P (mg/g)	0.457	0.298	0.307	0.238	0.415	0.295	0.317	0.355	35% reduction	33% reduction	48% reduction	9% reduction	36% reduction	30% reduction	22% reduction	< 0.100
		Al-bound P (mg/g)	0.097	0.170	0.331	0.216	0.342	0.308	0.225	0.248	75% increase	241% increase	123% increase	253% increase	218% increase	132% increase	157% increase	NA

Lakewide P mass increases were more modest in conjunction with the 2023 alum application (Fig. 16 and 17). Like other post-alum treatment years, P mass was greatest in the epilimnion versus hypolimnion (Fig. 17). This pattern suggested that algae might be assimilating P directly from sediment during inoculation into the water column. The lake-wide net internal P load during this period was 17 kg/d, which was lower than the 2022 estimate but higher compared to other alum application years (i.e., 2017, 2019, and 2021, Table 3 and Fig. 18).

Table 3. Summer net internal phosphorus loading ($P_{net\ int\ load}$) estimates (bold font) for Cedar Lake in 2010 (pretreatment) and 2017-23 (post-treatment).

Summer	Period (d)	$P_{tributary}$ (kg)	$P_{discharge}$ (kg)	$P_{retention}$ (kg)	$P_{lake\ storage}$ (kg)	$P_{net\ int\ load}$ (kg)	$P_{net\ int\ load}$ (kg/d)	$P_{net\ int\ load}$ (mg/m² d)
2010	97	445	238	207	3,931	**3,723**	**38**	**8.8**
2017	83	349	212	137	1,287	**1,150**	**14**	**3.2**
2018	87	292	128	164	2,288	**2,123**	**24**	**2.8**
2019	85	346	141	205	28	**-77**	**-1**	**0**
2020	112	456	369	87	1,434	**1,351**	**12**	**2.8**
2021[1]	84	293	84	210	614	**404**	**5**	**1.1**
2022	84	246	283	-37	3,066	**3,103**	**37**	**8.5**
	56[2]	164	68	96	923	**827**	**15**	**3.4**
	42[3]	123	175	-52	2,092	**2,144**	**51**	**11.7**
2023	56	[4]164	33	131	1,086	**955**	**17**	**3.9**

[1] $P_{tributary}$, $P_{discharge}$, and $P_{retention}$ are estimates for the period May through July only due to flow logger vandalism.

[2] Only for the period 5/23/22 to 7/18/22 - i.e., before the mid-summer turnover

[3] Only for the period 7/18/22 to 8/29/22 - i.e., after the mid-summer turnover

[4] Estimated from the summer 2022 due to logger failure in 2023

One of the concerns over aluminum sulfate application is removal of Fe from recycling as a result of treatment. Cedar Lake hypolimnetic total and dissolved Fe were low relative to SRP before treatment (James et al. 2015). The hypolimnetic total Fe:P ratio was only ~ 1.4:1 mass, indicating insufficient Fe to bind all of the hypolimnetic P during fall turnover and chemical oxidation of Fe to Fe(OOH). Thus, some of the soluble P was directly available for algal uptake and bloom formation during turnover.

Addition of aluminum sulfate can indirectly reduce hypolimnetic Fe by its reaction with S to form FeS, which is inert and becomes buried from further recycling. The sulfate byproduct of alum application is reduced by anaerobic bacteria in the profundal sediment to form S, which then reacts with Fe to form insoluble FeS.

Table 4. Mean summer bottom iron concentrations in Cedar Lake in 2010 (before Al) and in 2023 (after 4 Al applications).

JUN-AUG	Total Fe (mg/L)	Dissolved Fe (mg/L)
2010	1.06	0.54
2023	0.53	0.28

Bottom iron patterns in Cedar Lake in 2023 suggested that concentrations have declined from pretreatment values in 2010 (Fig. 19). Mean Jun-Aug bottom concentrations have declined by nearly 50% in 2023 compared to 2010 (Table 4).

Changes in sediment chemistry and anaerobic diffusive phosphorus flux

Interestingly, even though the 2023 alum application led to low concentration of P in the hypolimnion and modest lake P mass accumulation, laboratory-derived anaerobic P flux from sediment collected at the WQ station was high relative to other years (Fig. 20). Sediment cores were collected in September, approximately 2 months after the alum application. While anaerobic P flux was still much lower compared to pretreatment fluxes (representing a 57% reduction), rates need to be much lower and on the order of < 1.5 mg/m^2 d in order to meet WQ targets. Spatially, anaerobic P fluxes ranged between 3.3 mg/m^2 d and 9.4 mg/m^2 d at depths $>$ 25 ft (48% to 72% reduction) and between 4.4 mg/m^2 d and 8.3 mg/m^2 d within the 20-25-ft depth contour (42% to 70% reduction, Fig. 21). Mean anaerobic P fluxes were similar in the 2 alum treatment zones at 6.3 mg/m^2 d, representing a 64% reduction at depth > 25 ft and a 50% reduction for the 20-25-ft depth contour (Fig. 22).

Sediment profiles at the WQ station indicated that added alum was located in the upper 8 cm in the sediment core collected at the WQ station located roughly in the center of the lake at a depth > 25 ft (Fig. 23). Below 8 cm, Al concentrations declined to baseline at this station. The area-based Al concentration in the upper 8-cm at the WQ station was ~ 83 g/m^2, close to the theoretical ~ 120 g/m^2 applied to depths > 25 ft since 2017. Along the N-S transect running down the approximate center of the lake, mean Al concentrations in the upper 10 cm sediment layer were higher at stations located at depths > 25 ft versus CL 24, located between the 20 and 25-ft depth contour (Fig. 24). To date, ~ 68 g Al/m^2 have been applied to the 20-25-ft depth contour.

Spatial variations in redox-P and aluminum-bound P in the upper 10-cm sediment layer are shown in Fig. 25 for stations located in the recently alum-treated zone (i.e., depths > 25 ft) and the 20-ft to 25-ft depth zone. Overall, redox-P concentrations have generally declined as a result

of binding onto the Al floc layer while aluminum-bound P concentrations have generally increased, reflecting P bound to alum. Increases in aluminum-bound P have been greatest for sediments located at depths > 25 ft (Fig. 25). These patterns coincided with a greater mean aluminum-bound P concentration in the upper 10-cm sediment layer within the > 25-ft depth contour versus the mean within the 20-25-ft depth contour (Fig. 22).

At station WQ 2, vertical variations in sediment chemistry indicated continued binding of P onto the Al floc (Fig. 26). Aluminum-bound P concentrations were elevated in the upper 8-cm layer as of September 2023, compared to pretreatment concentrations. In contrast, concentrations of redox-P (i.e., sediment P that contributes to internal P loading) have declined in the surface sediment compared to the pretreatment concentration peaks (Fig. 26).

Conclusions and Recommendations

The 2023 alum treatment was largely successful in reducing the severity of cyanobacteria blooms after turnover in late-August. Application in mid-July substantially reduced the development of hypolimnetic P gradients immediately before turnover and, thus, any mixing of SRP into the water column for algal uptake. Unlike patterns in 2022, where SRP increased as a result of the late July turnover event, concentrations in August-September 2023 were generally below detection limits throughout most of the water column. However, some SRP availability was evident above the sediment-water interface before turnover, as the SRP concentration was 0.053 mg/L on 8 August 2023. Because hypolimnetic iron concentrations were low, some of this P was probably assimilated by cyanobacteria rather than precipitated with Fe(OOH) back to the sediment, resulting in a modest early September bloom.

In contrast, the 4th alum treatment did not appear to entirely suppress internal P loading in 2023 as some significant lakewide P mass increase was observed (i.e., Fig. 16 and 18). In particular, lakewide P mass accumulation was relatively high compared to other treatment years (Fig. 18). For instance, it was 1,150 kg/summer, -177 kg/summer, and 404 kg/summer during the 2017, 2019, and 2021 treatment years, respectively, and 955 kg/summer in 2023. In addition, laboratory-derived anaerobic diffusive P flux was higher relative to other treatment years (i.e.,

Fig. 20). These trends suggest that as of the 4th alum treatment, the Al floc layer is still not entirely controlling diffusive P flux from anaerobic sediment. Thus, in combination with low dissolved iron accumulation in the hypolimnion, internal P loading, although much lower versus pretreatment rates, is still driving cyanobacteria blooms in Cedar Lake.

Total and dissolved iron concentrations above the sediment-water interface were also ~ 0.5X lower in 2023 compared to the pretreatment year 2010 (i.e., Table 4 and Fig. 19). This trend supported an hypothesis that sulfate diffusion (a biproduct of aluminum sulfate application) into the sediment and metabolic reduction to S by anaerobic bacteria, might have led to the formation of iron sulfide ($FeS_{(solid)}$) and removal from further recycling. The ratio of iron to phosphorus in the hypolimnion was low before the initiation of alum application (DFe:SRP ratio = 0.9:1 mass in 2010). Thus, during turnover and reoxygenation of the hypolimnion, there was not enough iron (chemically converted to iron oxyhydroxide – Fe(OOH)) to precipitate all of the soluble P, resulting in P availability for cyanobacteria uptake.

Interestingly, even though total and dissolved Fe concentrations declined in the bottom waters in 2023 relative to the pretreatment year 2010, Bottom SRP concentrations were also lower in 2023, resulting in a higher DFe:SRP ratio in 2023. Thus, the 2023 DFe:SRP mass ratio after the alum treatment (i.e., date range = 8/8 to 10/16) actually improved to 2.9:1 mass. However, there was still not enough iron stoichiometrically to precipitate out all hypolimnetic SRP during the 2023 turnover. Gunnars et al. (2002) experimentally determined that a mass ratio > 3.6:1 was needed to completely adsorb P onto Fe(OOH). This stoichiometric Fe:P ratio imbalance in 2023 and, thus, some SRP availability after the late August turnover, could explain the development of the modest algal bloom in 2023.

These results suggest that for Cedar Lake, both anaerobic diffusive P flux suppression and balancing the Fe:P ratio so that it is > ~ 4:1 is needed to successfully control internal P loading. Specifically, anaerobic diffusive P flux still needs to be reduced substantially in both treatment zones (i.e., Fig. 22) to attain WQ goals. In addition, hypolimnetic Fe concentrations need to increase relative to hypolimnetic P to maintain the Fe:P mass ratio at >4:1. This balance can be achieved via a couple of options: 1) by continuing to reduce internal P loading and SRP

concentrations in the hypolimnion relative to Fe, and 2) by supplemental Fe addition to maintain the Fe:P ratio > 4. A combination of these two options would work also.

The 2024 nontreatment year results will be important in making decisions regarding future internal P loading management in Cedar Lake. As in other nontreatment years, will anaerobic diffusive P flux rebound (i.e., increase) or will the $Al(OH)_3$ floc layer built up over 4 application cycles suppress internal P loading? If anaerobic diffusive P flux increases in 2024 relative to hypolimnetic iron, expect cyanobacteria bloom occurrence after turnover.

References

APHA (American Public Health Association). 2011. Standard Methods for the Examination of Water and Wastewater. 22th ed. American Public Health Association, American Water Works Association, Water Environment Federation.

Avnimelech Y, Ritvo G, Meijer LE, Kochba M. 2001. Water content, organic carbon and dry bulk density in flooded sediments. Aquacult Eng 25:25-33.

Boström B. 1984. Potential mobility of phosphorus in different types of lake sediments. Int. Revue. Ges. Hydrobiol. 69:457-474.

de Vicente I, Huang P, Andersen FØ, Jensen HS. 2008. Phosphate adsorption by fresh and aged aluminum hydroxide. Consequences for lake restoration. Environ Sci Technol 42:6650-6655.

Egemose SG, Wauer G, Kleeberg A. 2009. Resuspension behavior of aluminum treated lake sediments: effects of aging and pH. Hydrobiologia 636: 203-217.

Egemose SG, Reitzel K, Andersen FØ, Jensen HS. 2013. Resuspension-mediated aluminum and phosphorus distribution in lake sediments after aluminum treatment. Hydrobiologia 701: 79-88.

Håkanson L, Jansson M. 2002. Principles of lake sedimentology. The Blackburn Press, Caldwell, NJ USA.

Hjieltjes AH, Lijklema L. 1980. Fractionation of inorganic phosphorus in calcareous sediments. J Environ Qual 8: 130-132.

Hondzo M, Feyaerts T, Donovan R, O'Connor BL. 2005. Universal scaling of dissolved oxygen distribution at the sediment-water interface: A power law. Limnol Oceanogr 50:1667-1676.

Huser BJ. 2017. Aluminum application to restore water quality in eutrophic lakes: maximizing

binding efficiency between aluminum and phosphorus. Lake Reserv Manage 33: 143-151.

James WF. 2012. Limnological and aquatic macrophyte biomass characteristics in Half Moon Lake, Eau Claire, Wisconsin, 2012: Interim letter report. University of Wisconsin – Stout, Sustainability Sciences Institute – Discovery Center, Menomonie, WI.

James WF. 2014. Phosphorus budget and management strategies for Cedar Lake, WI. University of Wisconsin – Stout, Sustainability Sciences Institute – Discovery Center, Menomonie, WI.

James WF. 2017. Phosphorus binding dynamics in the aluminum floc layer of Half Moon Lake, Wisconsin. Lake Reserv Manage 33:130-142.

James WF, Bischoff JM. 2020. Sediment aluminum:phosphorus binding ratios and internal phosphorus loading characteristics 12 years after aluminum sulfate application to Lake McCarrons, Minnesota. Lake Reserv Manage 36:1-13.

James WF, PW Sorge, PJ Garrison. 2015. Managing internal phosphorus loading in a weakly stratified eutrophic lake. Lake Reserv Manage 31:292-305.

Mortimer CH. 1971. Chemical exchanges between sediments and water in the Great Lakes – Speculations on probable regulatory mechanisms. Limnol Oceanogr 16:387-404.

Nürnberg GK. 1988. Prediction of phosphorus release rates from total and reductant-soluble phosphorus in anoxic lake sediments. Can J Fish Aquat Sci 45:453-462.

Nürnberg GK. 2009. Assessing internal phosphorus load – Problems to be solved. Lake Reserv Manage 25:419-432.

Pilgrim KM, Huser BJ, Brezonik PL. 2007. A method for comparative evaluation of whole-lake and inflow alum treatment. Wat Res. 41:1215-1224.

Psenner R, Puckso R. 1988. Phosphorus fractionation: Advantages and limits of the method for the study of sediment P origins and interactions. Arch Hydrobiol Biel Erg Limnol 30:43-59.
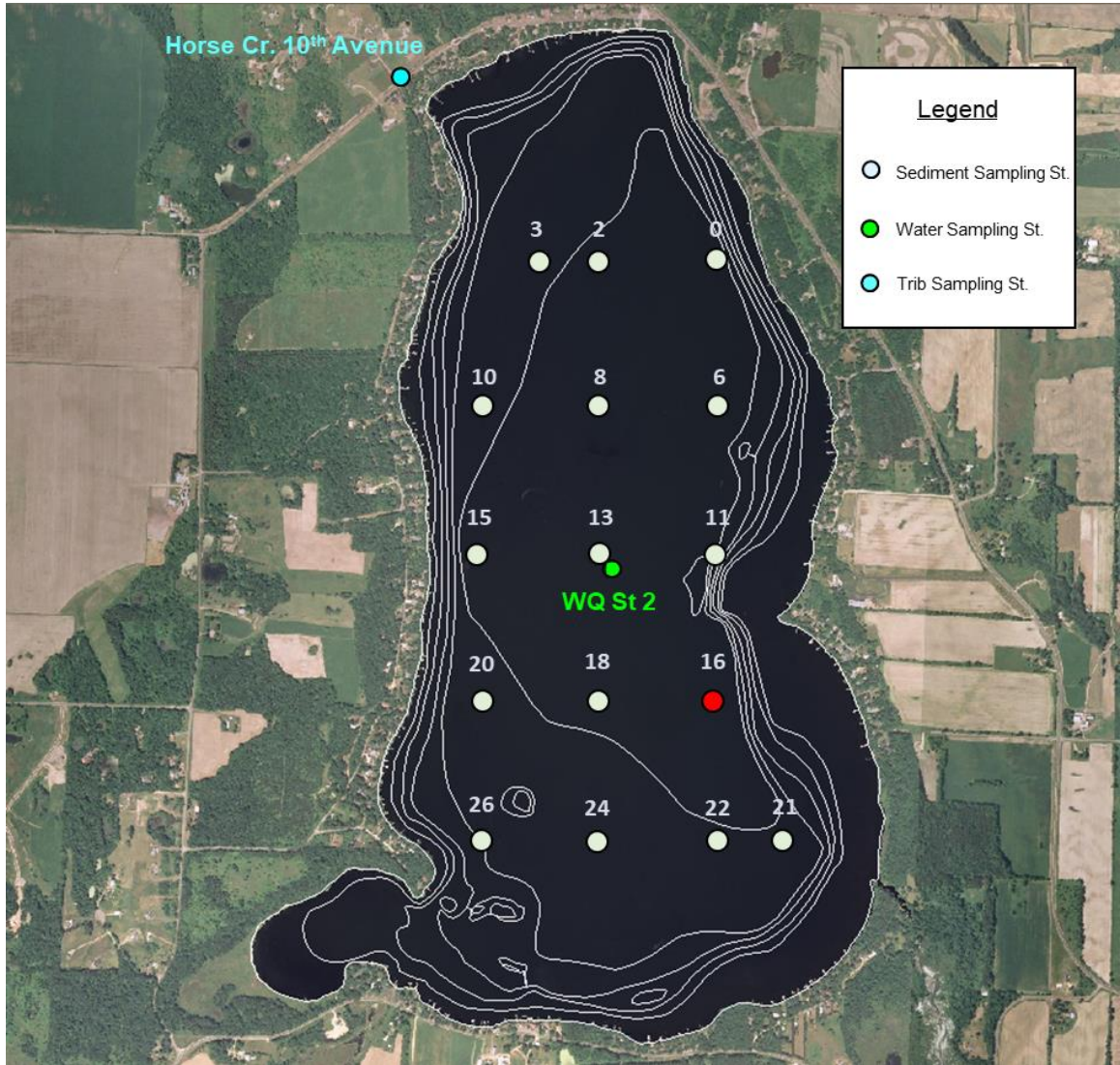
Figure 1. Sediment and water sampling stations in 2023. There was not enough sediment for analysis from the cores collected at Station 16.
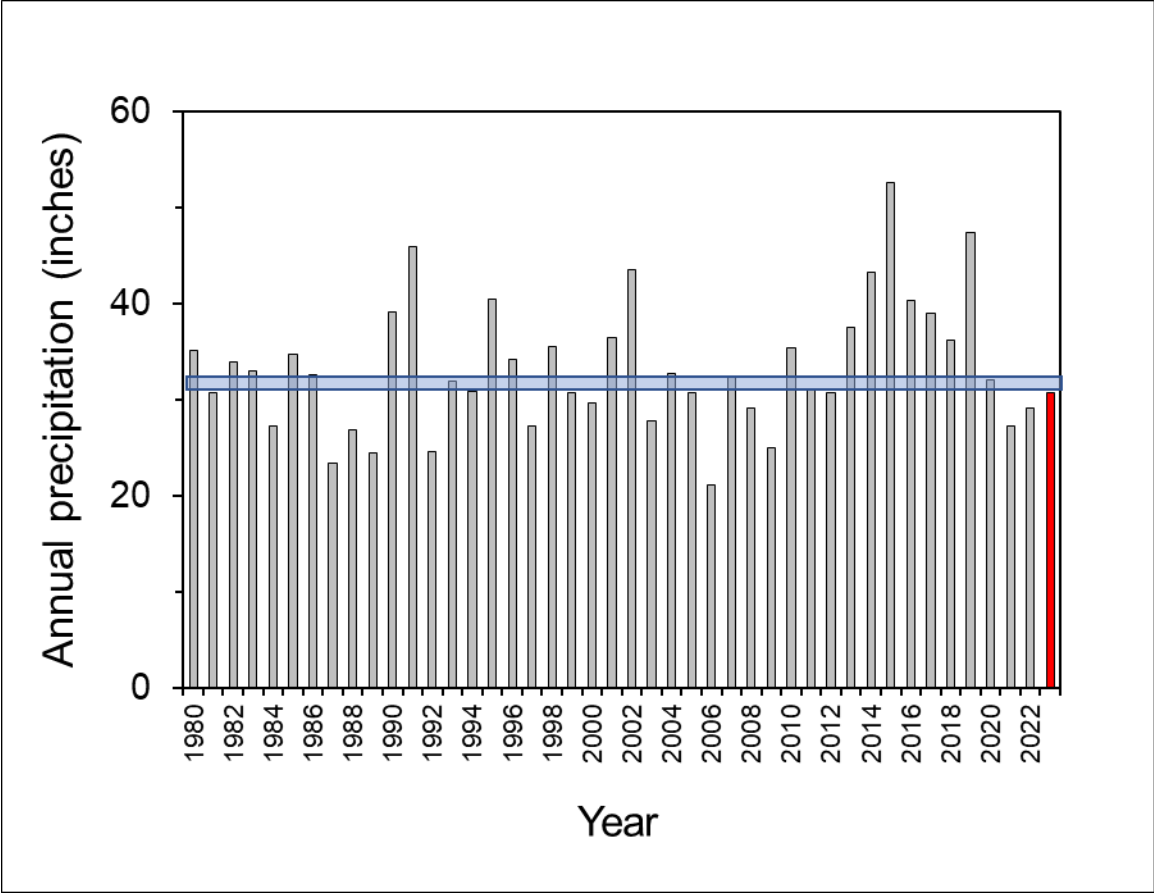
Figure 2. Variations in annual precipitation at Amery, WI. Blue horizontal line represents the average. The year 2023 is highlighted in red.
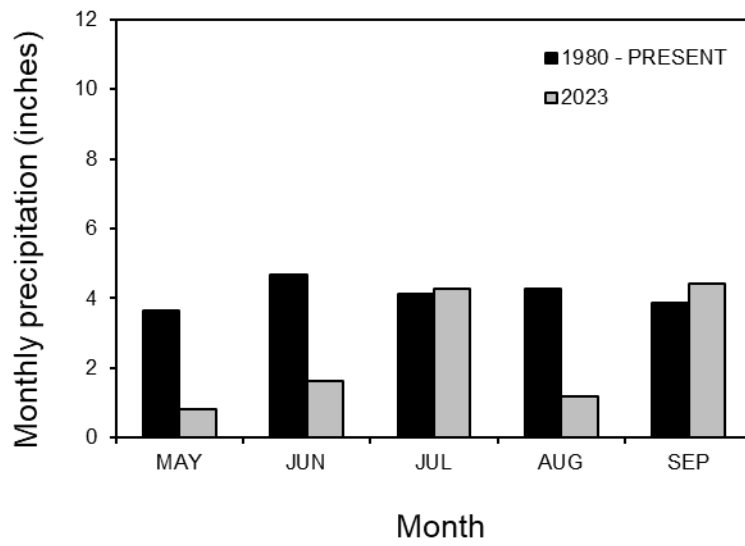
Figure 3. A comparison of average monthly precipitation.
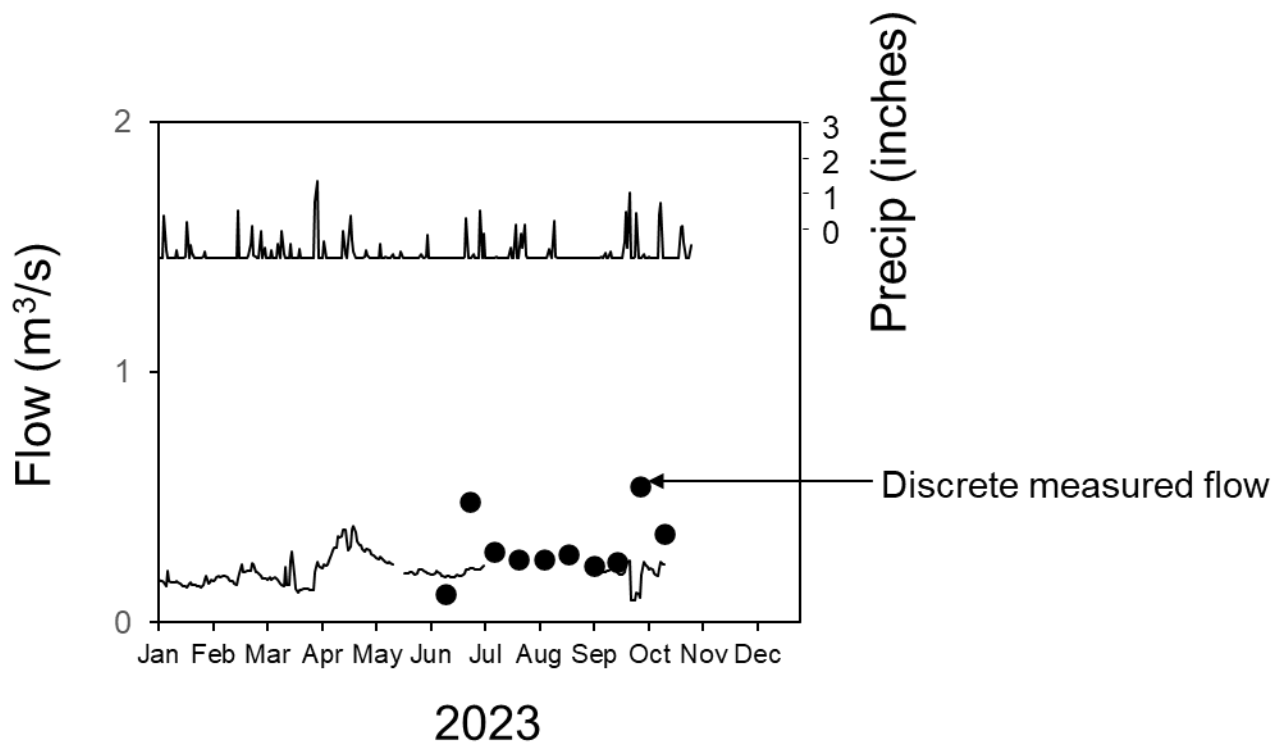
Figure 4. Seasonal variations in daily precipitation at Amery, WI, and flow for Horse Creek at 10th Ave.
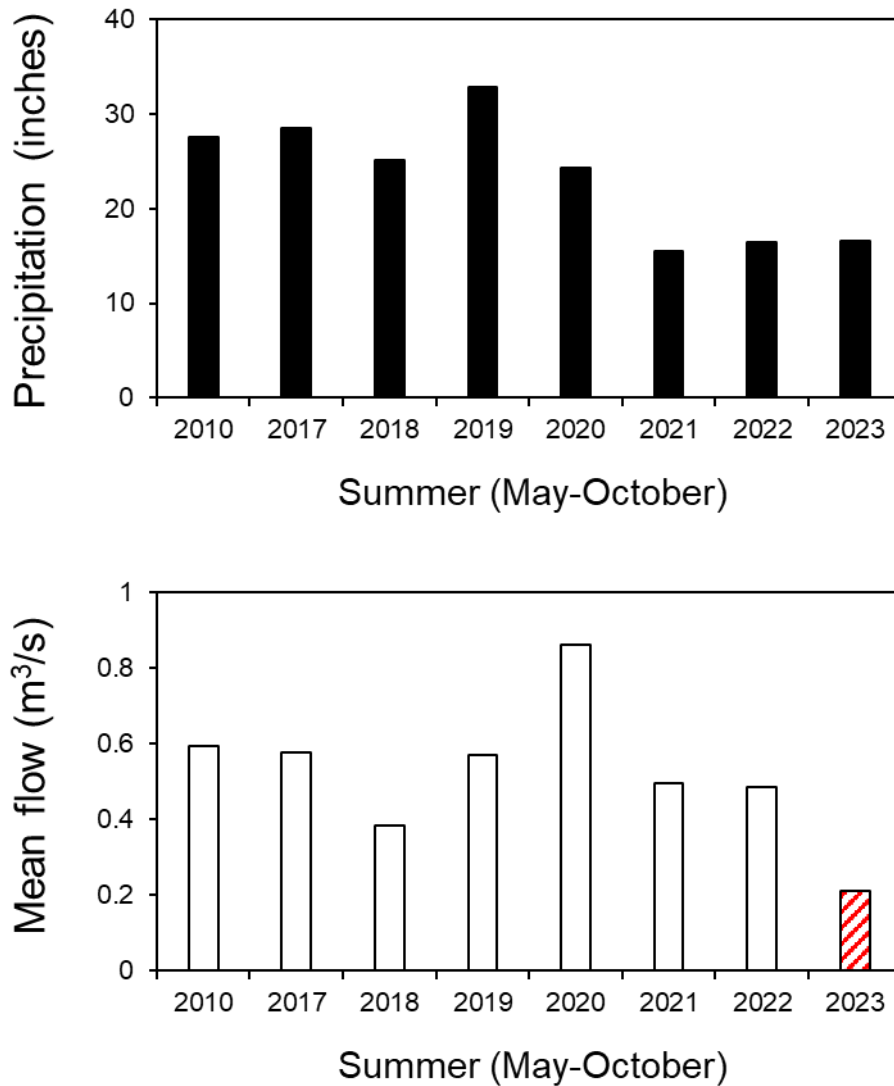
Figure 5. A comparison of summer (May-October) precipitation (upper panel) and mean Horse Creek flow (lower panel). The summer of 2010 was a pretreatment year. Alum was applied to the lake in late June 2017, 2019, 2021, and 2023. The mean flow for 2023 is probably an underestimate due to logger failure.
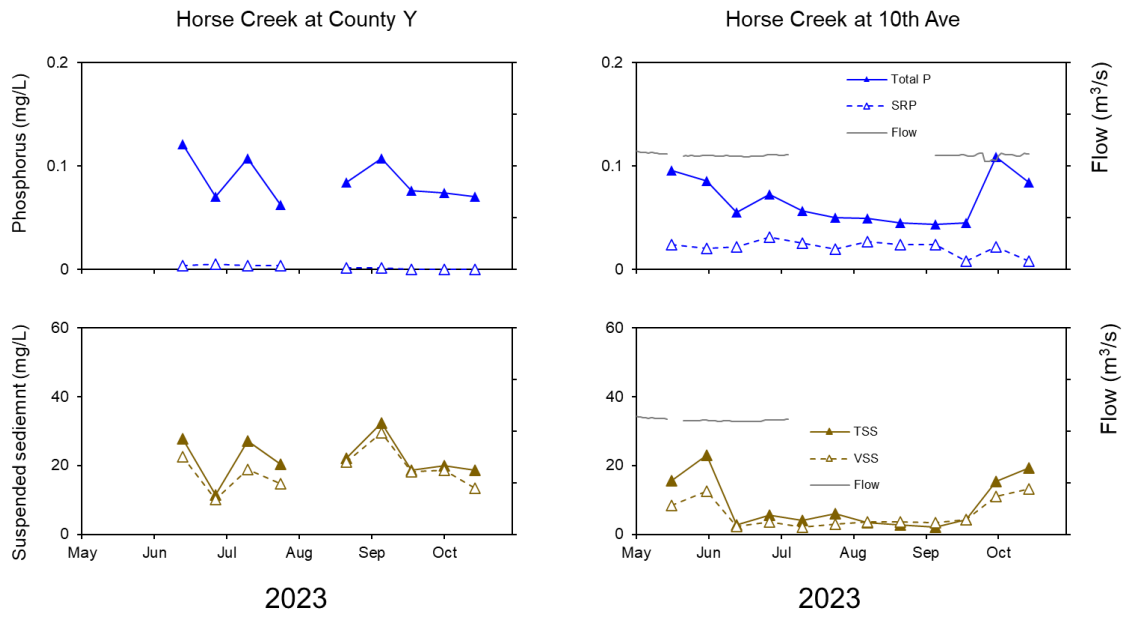
Figure 6. Seasonal variations in total phosphorus (P) and soluble reactive P (SRP) concentration at Horse Creek County Y (i.e., below Horse Lake) and 10th Ave (i.e., mouth to Cedar Lake).
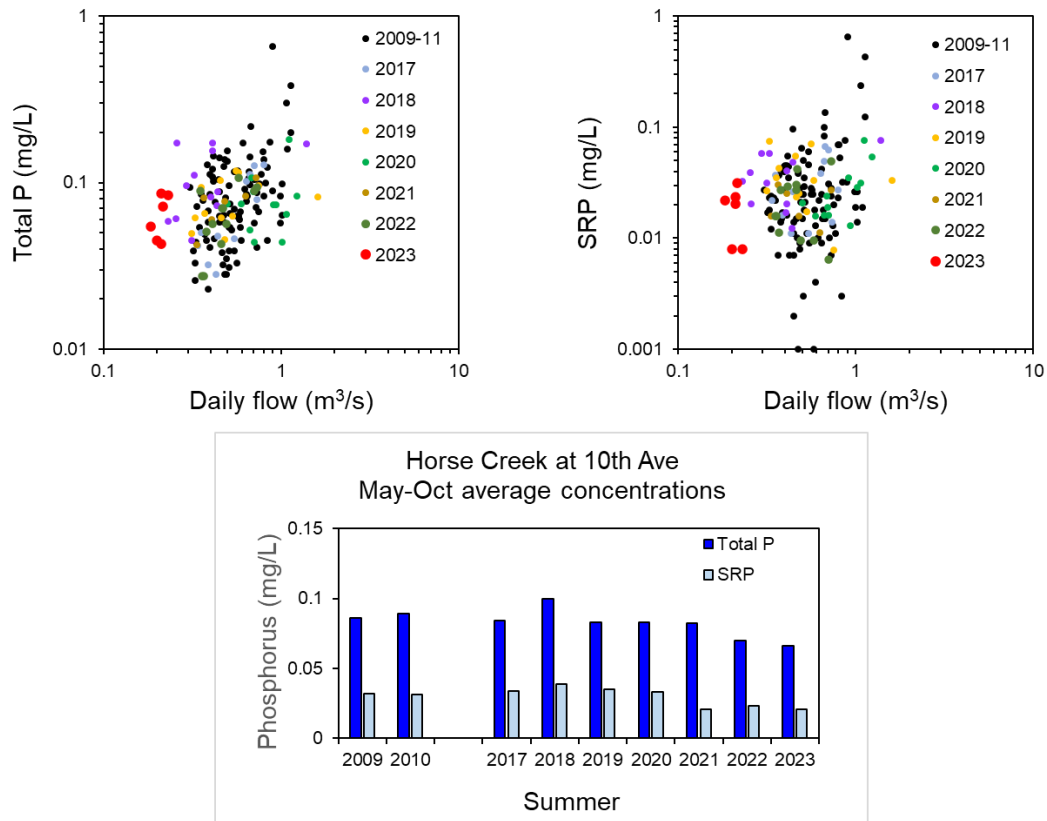
Figure 7. Phosphorus (P) concentration versus daily flow at Horse Creek at 10th Ave. Flows may be underestimated for 2023 due to logger failure.
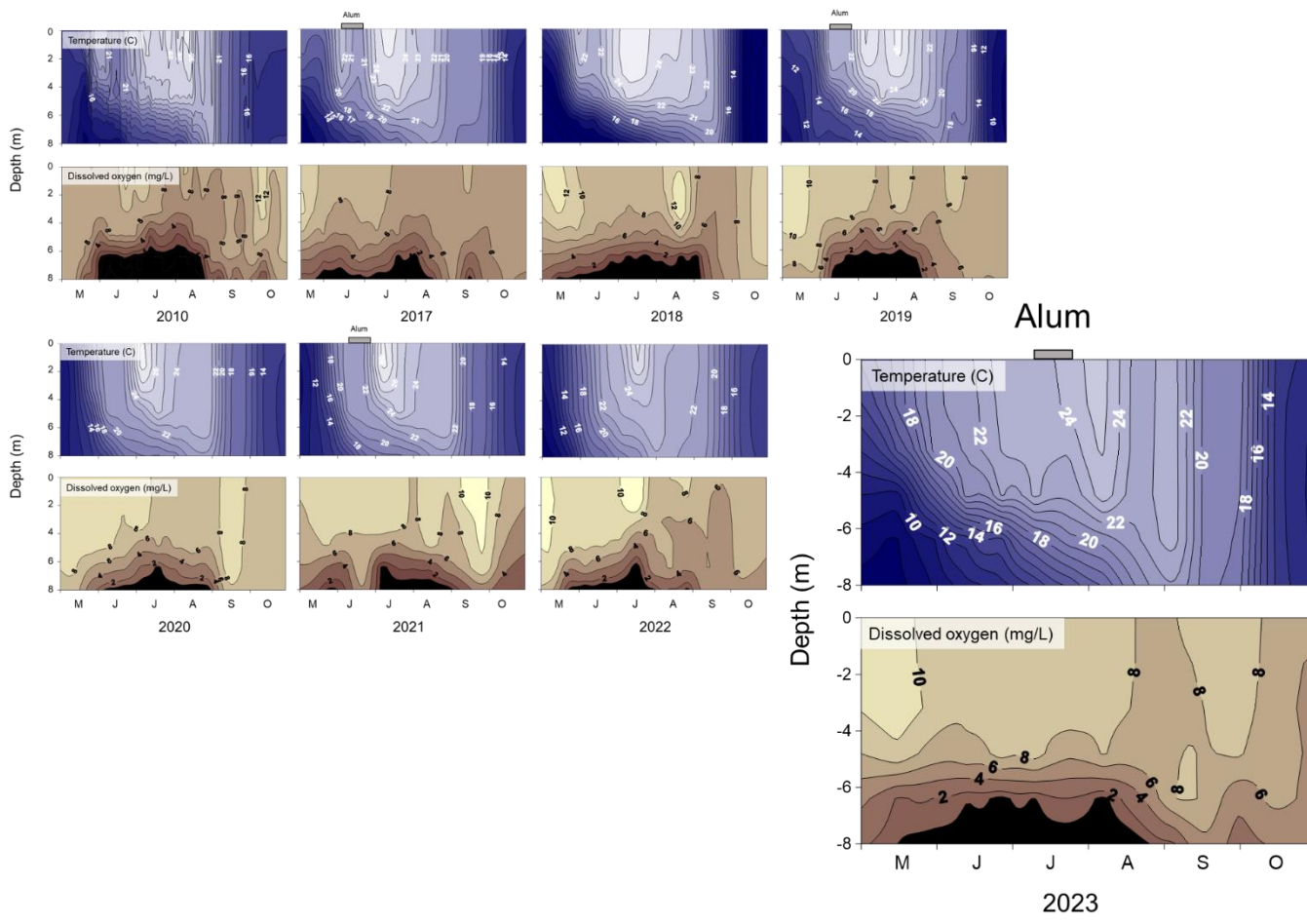
Figure 8. Seasonal and vertical variations in temperature (upper panels) and dissolved oxygen (lower panels) in 2010 (pre-treatment) and 2017-2023 (after alum treatment). Alum was applied in June 2017, 2019, 2021, and 2023.

Figure 9. Seasonal variations in bottom (i.e., ~ 0.25 m above the sediment-water interface) total phosphorus (P), and bottom soluble reactive P (SRP) during a pretreatment year (2010) and the post-alum treatment years 2017-23. Alum was applied in June 2017, 2019, 2021, and 2023.
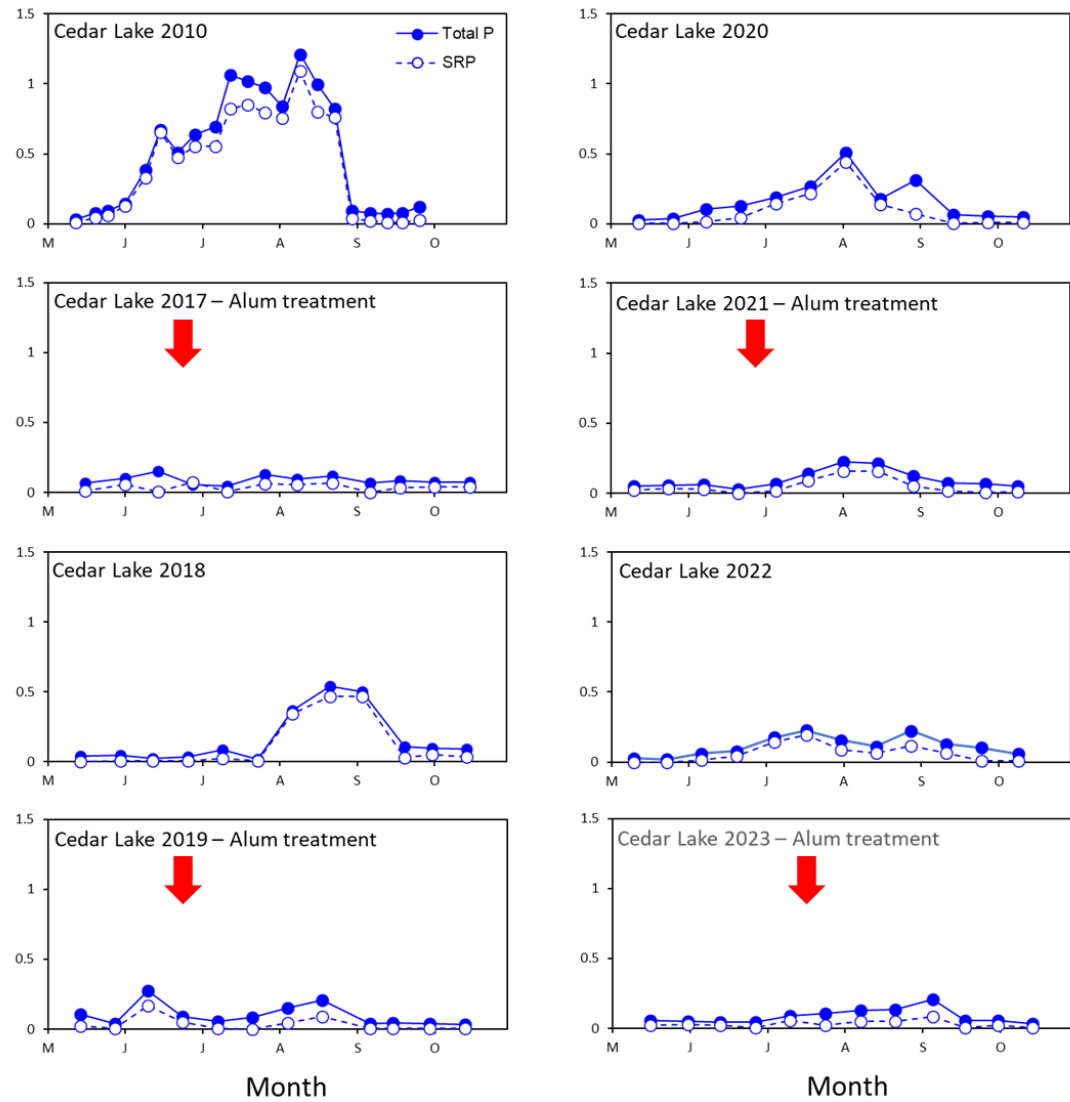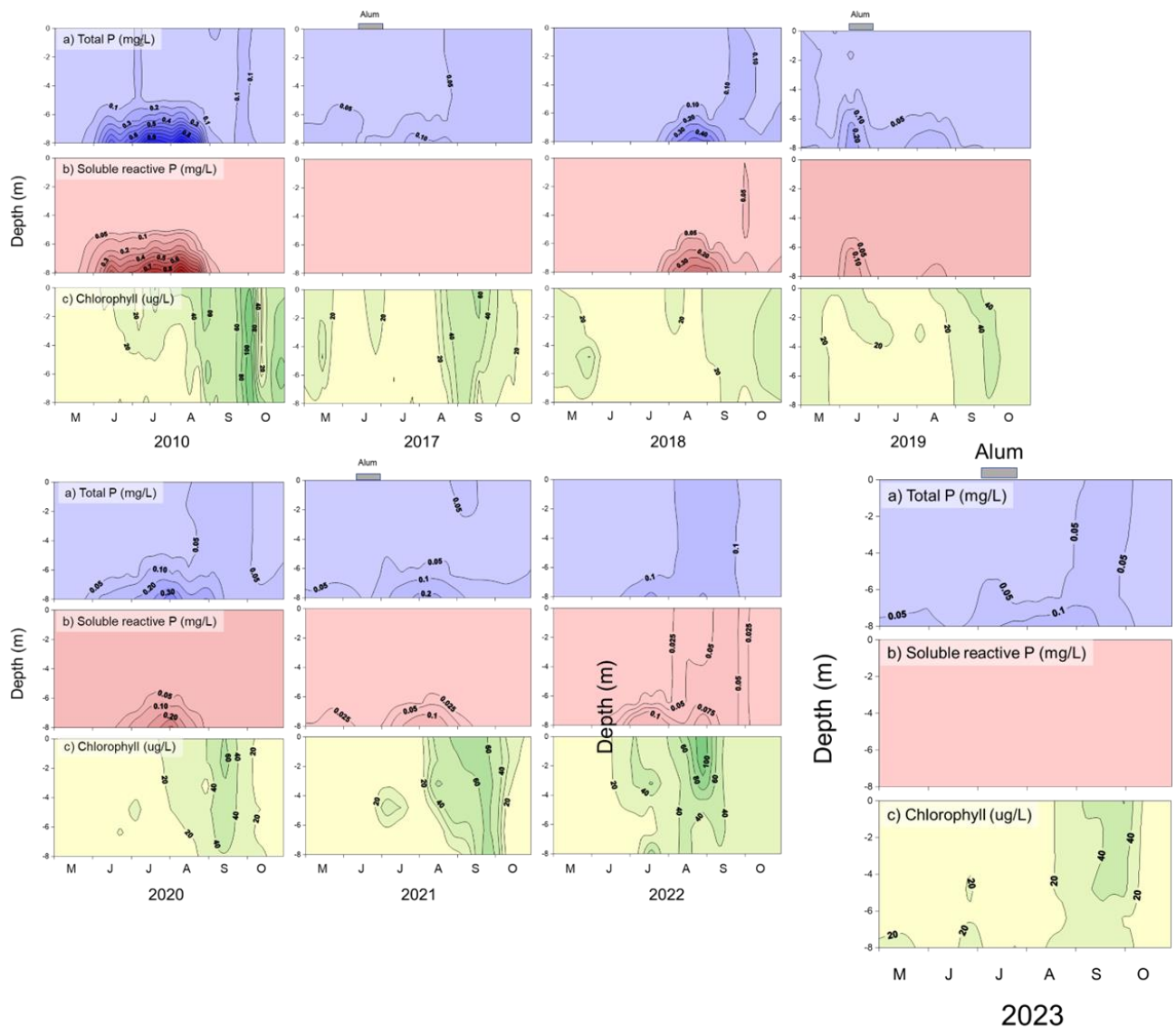
Figure 10. Seasonal and vertical variations in a) total phosphorus (P), b) soluble reactive P, and c) chlorophyll in 2010 (pretreatment) versus 2017-23 (post-treatment). Alum was applied in June 2017, 2019, 2021, and 2023.
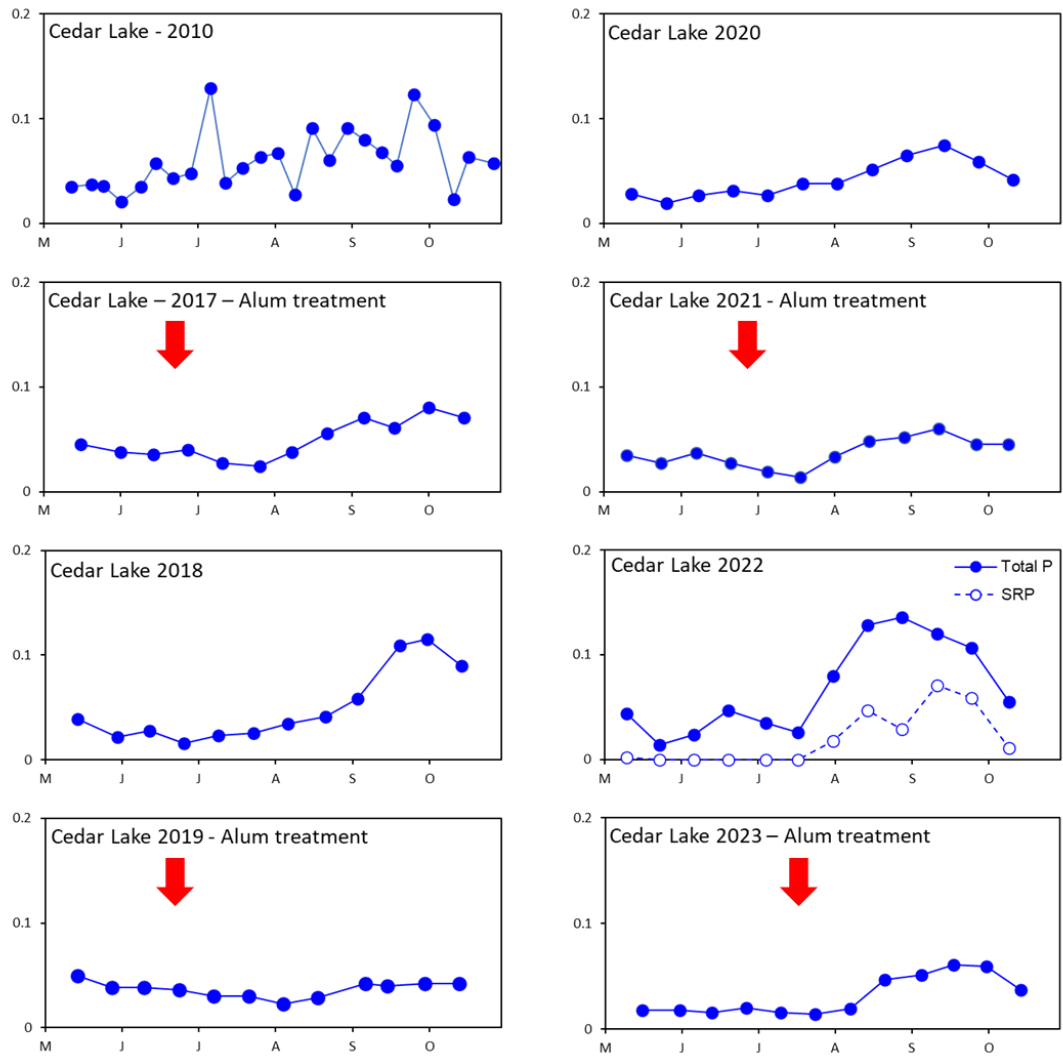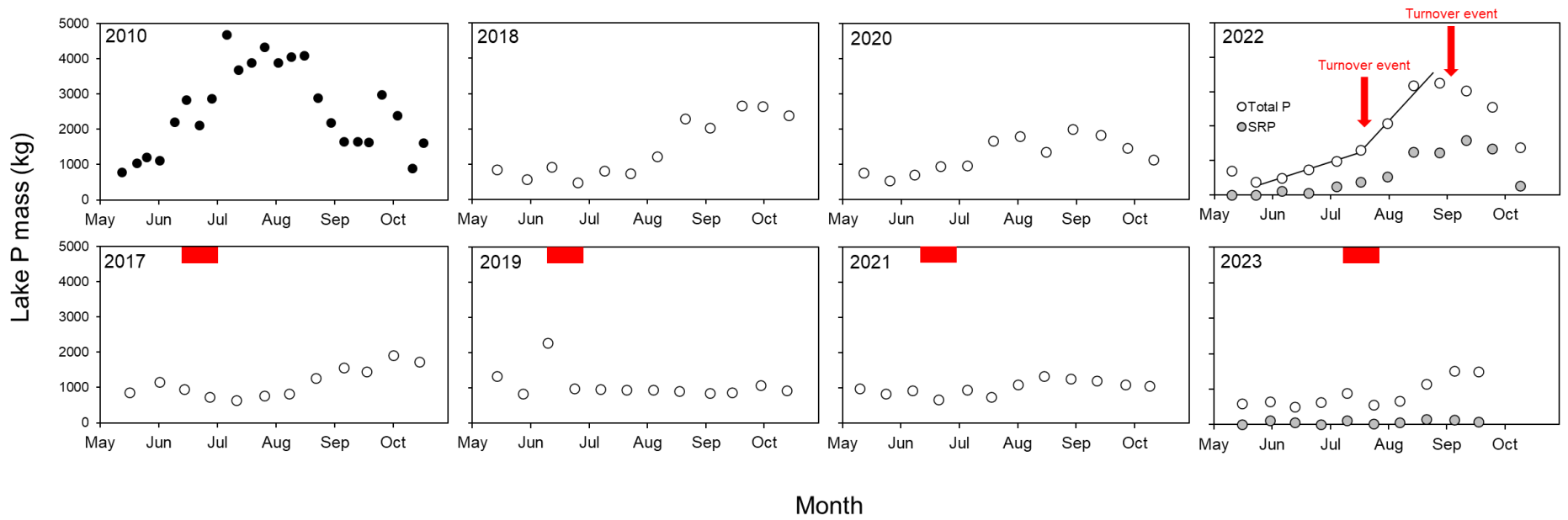
Figure 11. Seasonal variations in surface total phosphorus (P), during a pretreatment year (2010) and the post-alum treatment years 2017-23. Alum was applied in June 2017, 2019, 2021, and 2023.
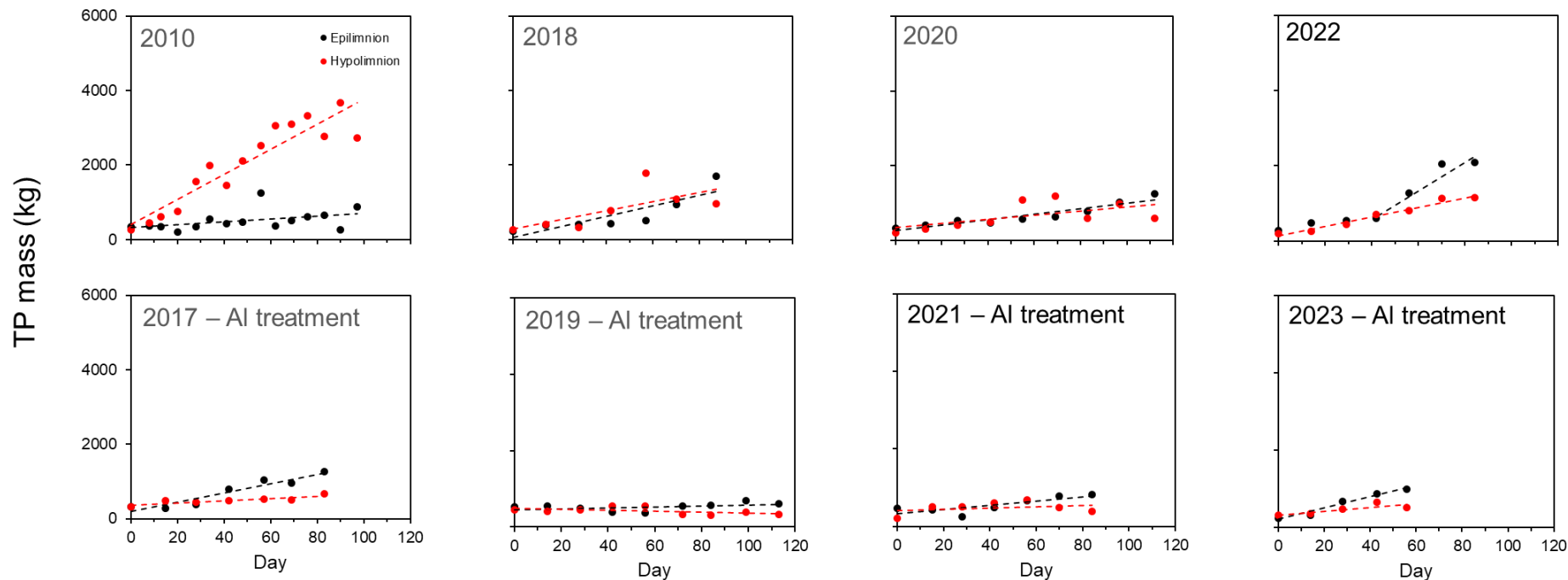
27

Figure 12. Seasonal variations in
surface chlorophyll during a
pretreatment year (2010) and the
post-alum treatment years 2017-23.
Alum was applied in June 2017,
2019, 2021, and 2023.
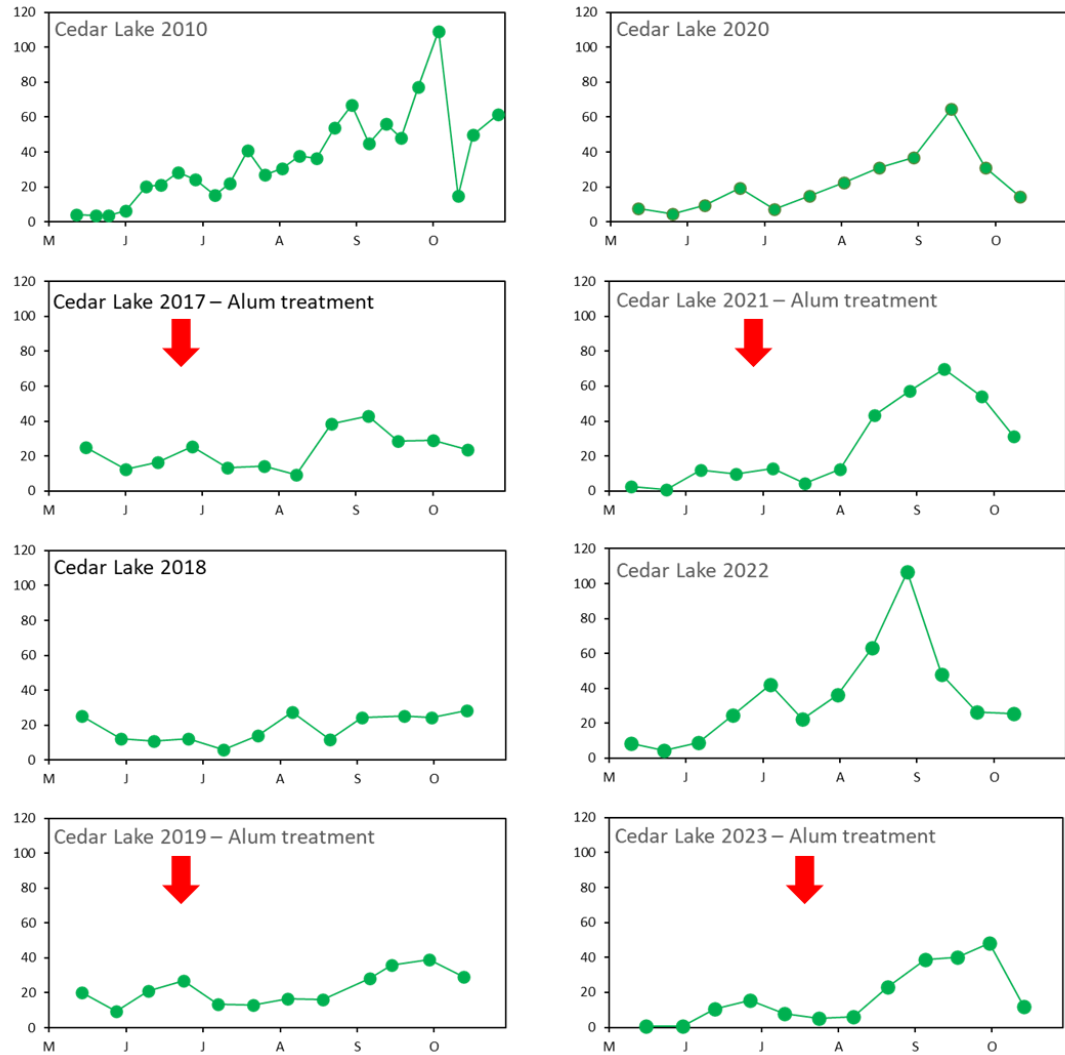
Secchi transparency (m)
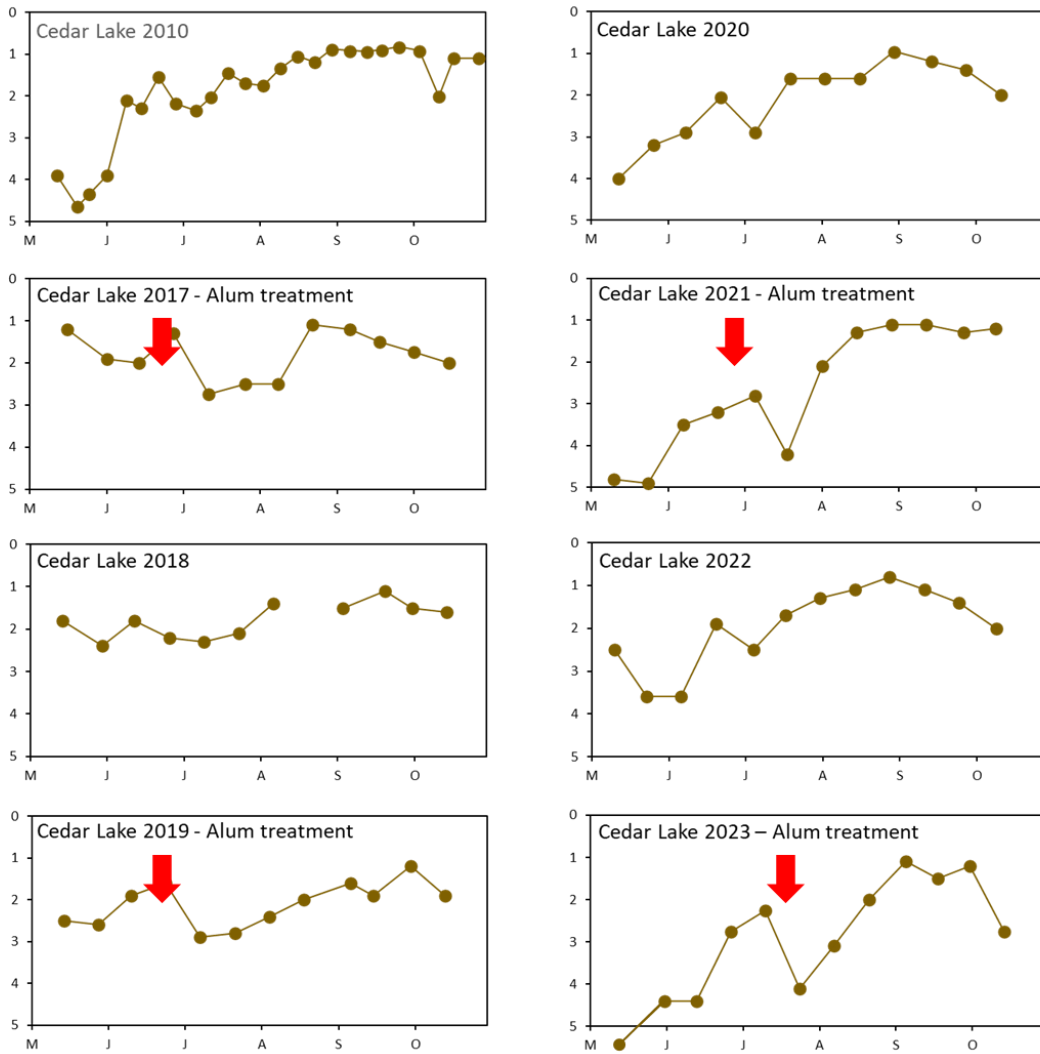
Figure 13. Seasonal variations in Secchi transparency during a pretreatment year (2010) and the post-alum treatment years 2017-23. Alum was applied in June 2017, 2019, 2021, and 2023.

Figure 14. Relationships between Secchi transparency and chlorophyll (upper panel) and total phosphorus (P) versus chlorophyll (lower panel) during the summer 2017-2023.
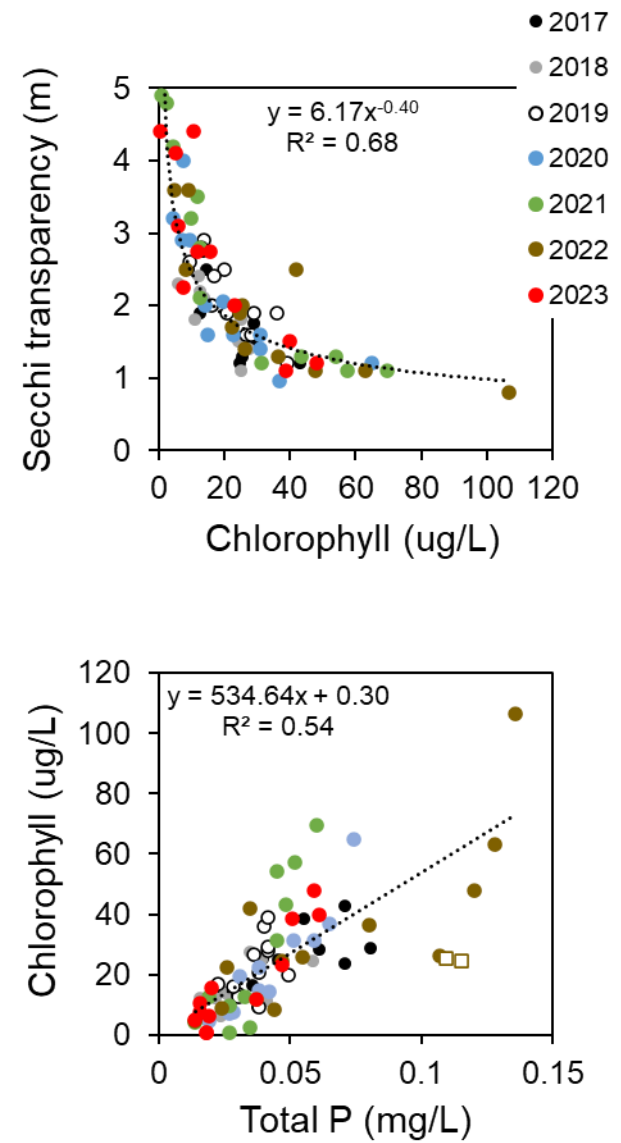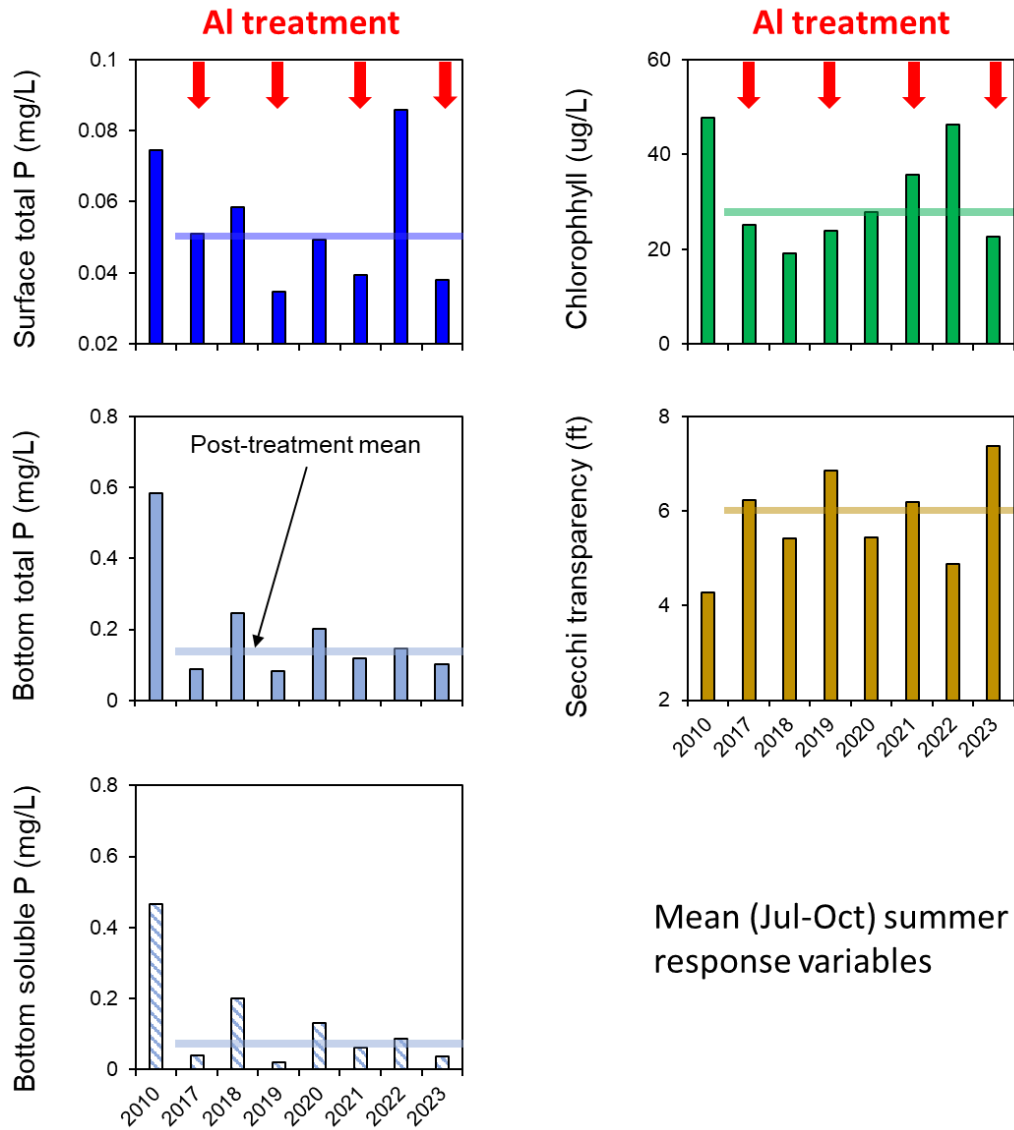
Figure 15. A comparison of mean summer (July-early October) summer concentrations of surface and bottom total phosphorus (P) and soluble reactive P (SRP), chlorophyll and Secchi transparency during a pretreatment year (2010) and the post-treatment years 2017-23. Alum was applied in June 2017, 2019, 2021, and 2023. Horizontal lines denote overall post-treatment means (2027-2023).

Mean (Jul-Oct) summer response variables

31

Figure 16. Seasonal variations in total phosphorus (P) mass during a pretreatment year (2010) and the post-treatment years 2017-23. Alum was applied in June 2017, 2019, 2021, and 2023.

Figure 17. Seasonal variations in total phosphorus (P) mass in the epilimnion (i.e., 0-4 m) and hypolimnion (> 4 m) during a pretreatment year (2010) and the post-treatment years 2017-23. Alum was applied in June 2017, 2019, 2021, and 2023.

Figure 18. Variations in lake phosphorus (P) mass accumulation before (2010) and after 1st through 4th alum application.
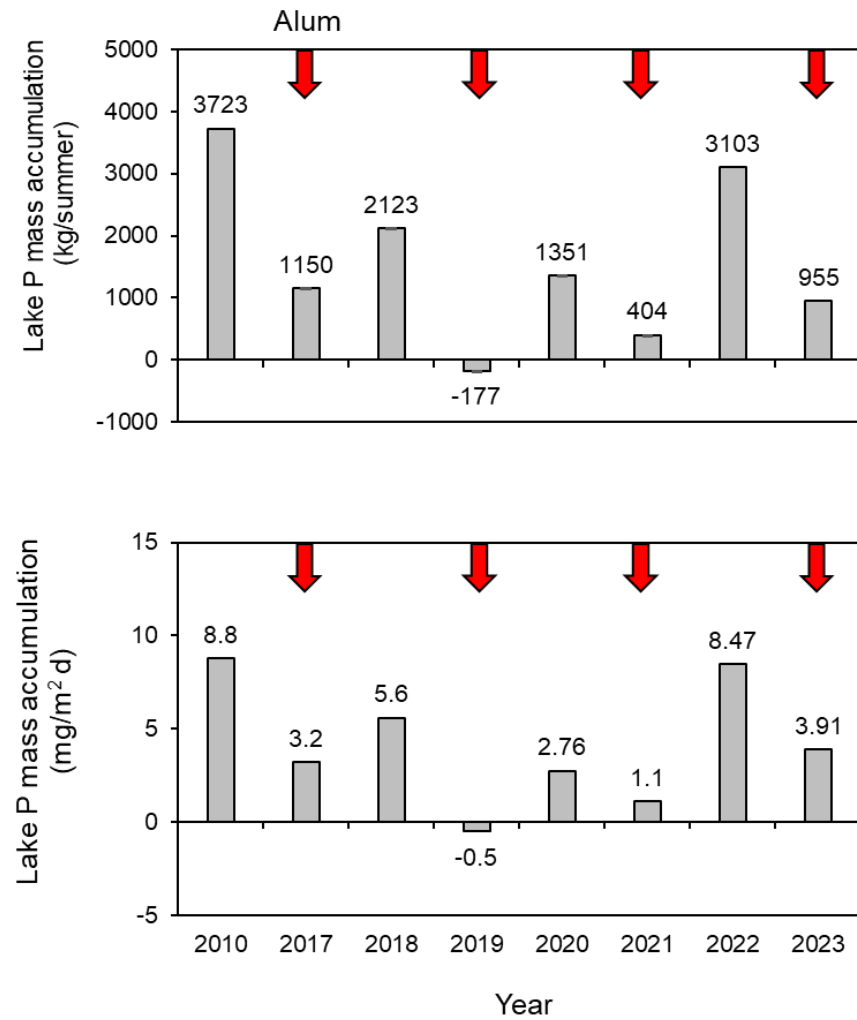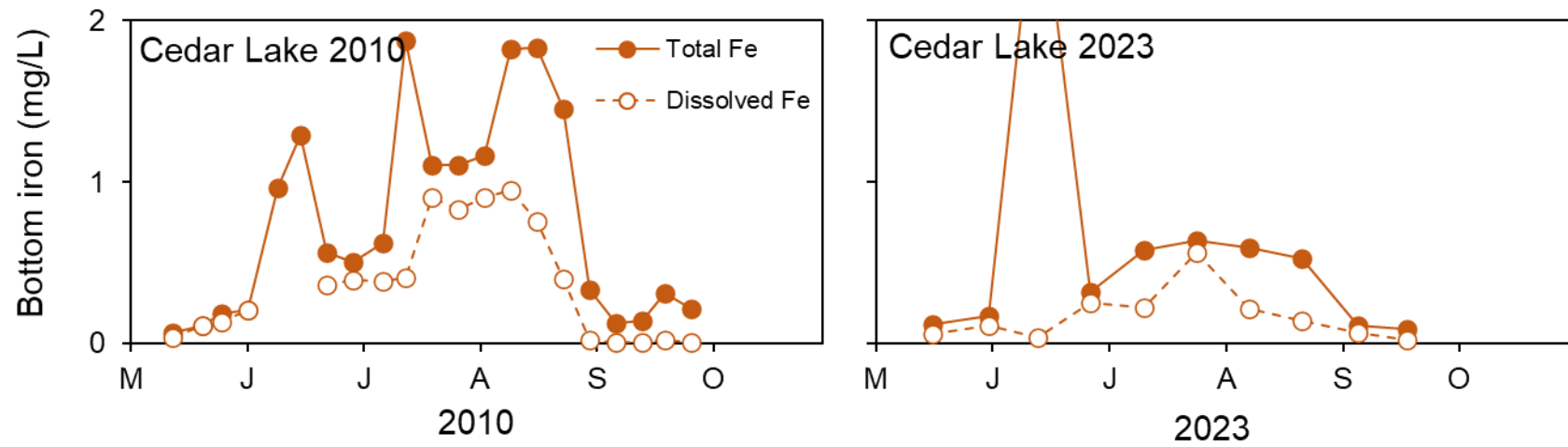
Figure 19. Variations in total and dissolved iron (Fe) at the lake bottom in 2010 (i.e., before Al applications) and 2023 (i.e., after the 4th Al application.
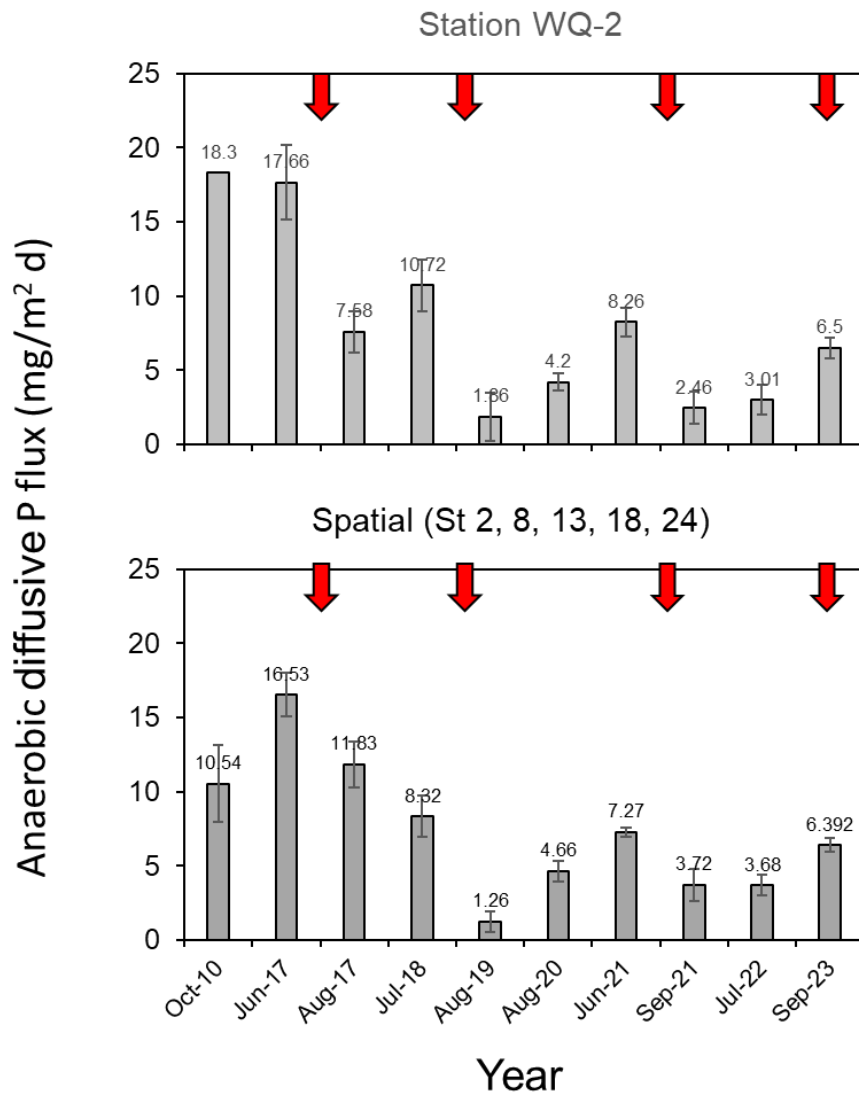
Figure 20. Variations in anaerobic diffusive phosphorus (P) flux (mg/m² d) before (June 2010 and 2017) and after the 1st through 4th alum application. WQ-2 = the centrally-located water quality sampling station. Spatial = the means from stations 3, 8, 13, 18, and 24 (see Fig. 1)

June 2017　　September 2023　　% Reduction

Anaerobic diffusive P flux (mg/m² d)
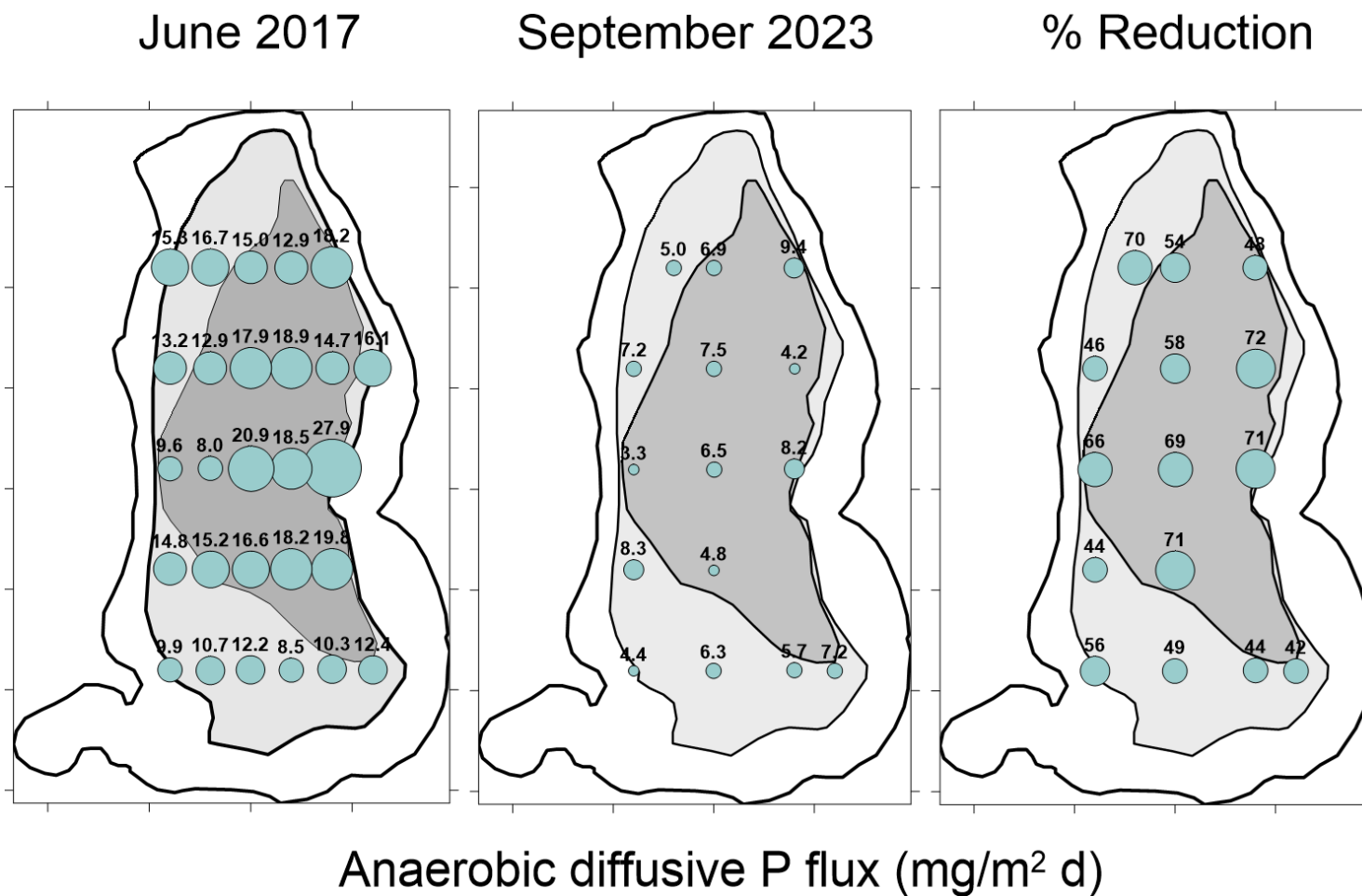
Figure 21. A comparison of spatial variations in laboratory-derived anaerobic diffusive P flux from sediment immediately before the initial alum treatment in 2017 (left), after the 4th alum application in 2023 (center), and percent improvement or reduction as of 2023 (right).
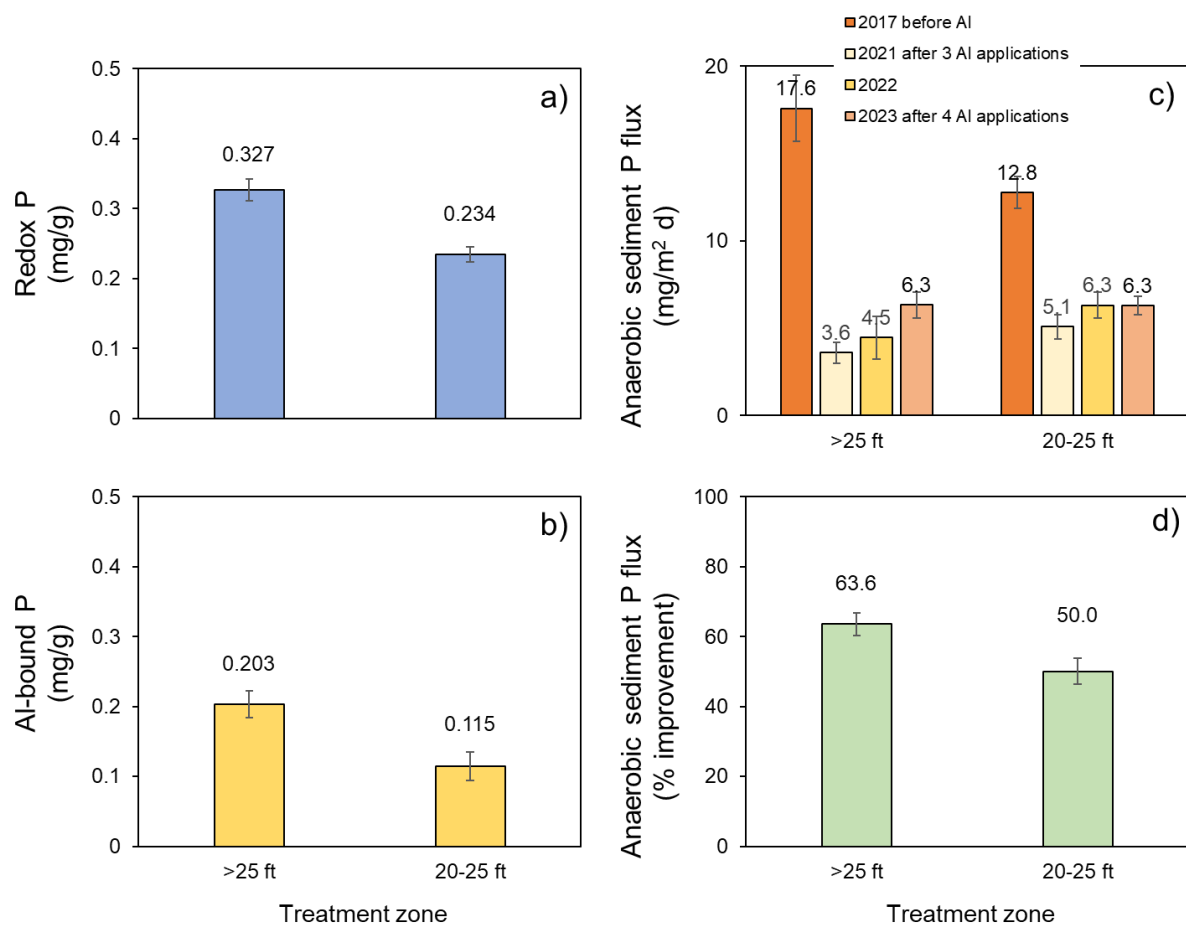
Figure 22. Mean redox P (a), aluminum-bound P (b), laboratory-derived anaerobic diffusive P flux (c), and anaerobic P flux percent improvement or reduction in 2023 (d) in the > 25-ft depth contour treatment zone (n=8) versus the 20-ft to 25-ft depth contour treatment zone (n=7).
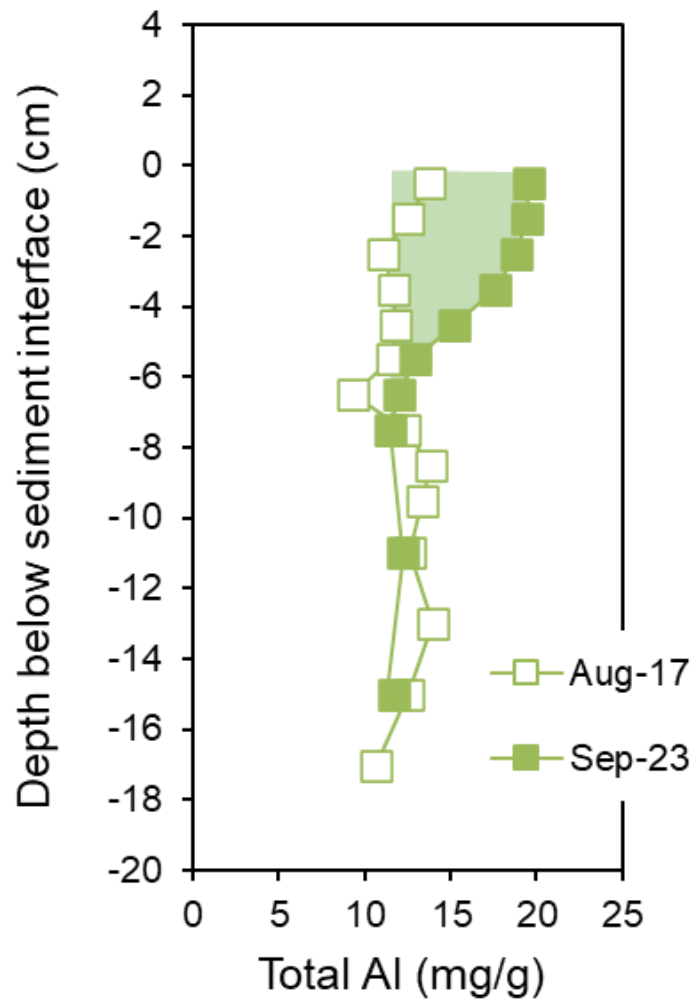
Figure 23. Vertical variations in total aluminum (Al) concentrations for a sediment core collected from station WQ2 (Figure 1) The sediment profile represents post-alum treatment conditions after three alum applications (2017, 2019, 2021, and 2023). Green shaded area denotes the Al floc layer concentration increase since the first alum application in 2017.
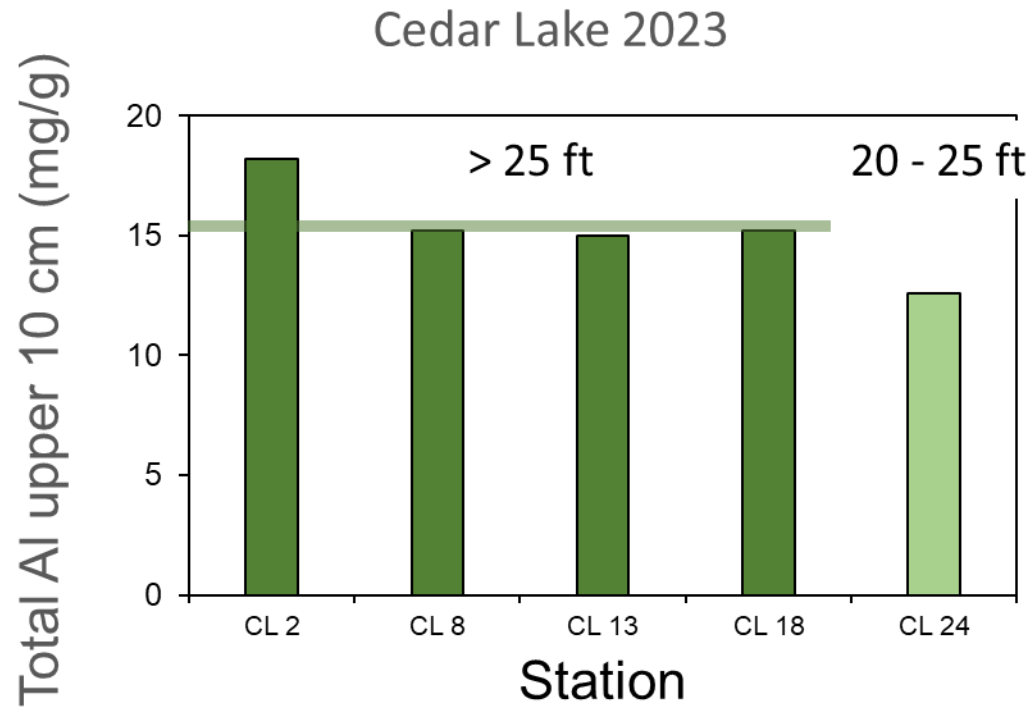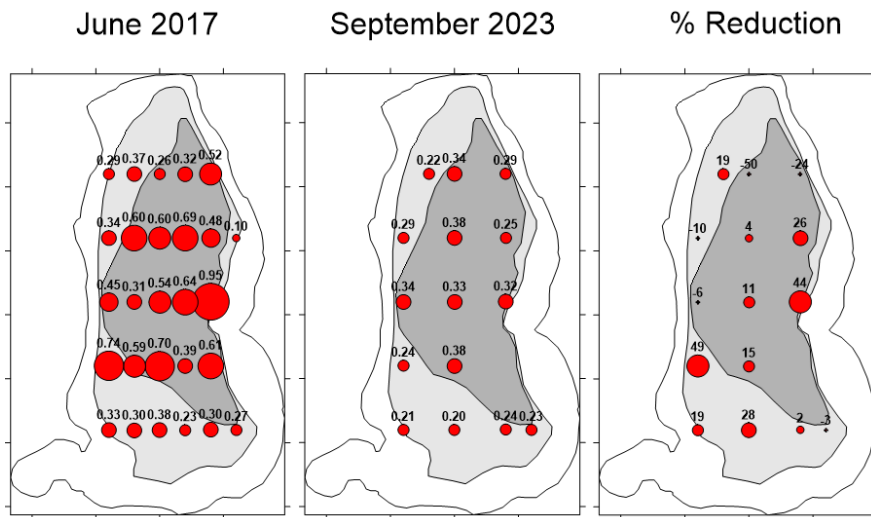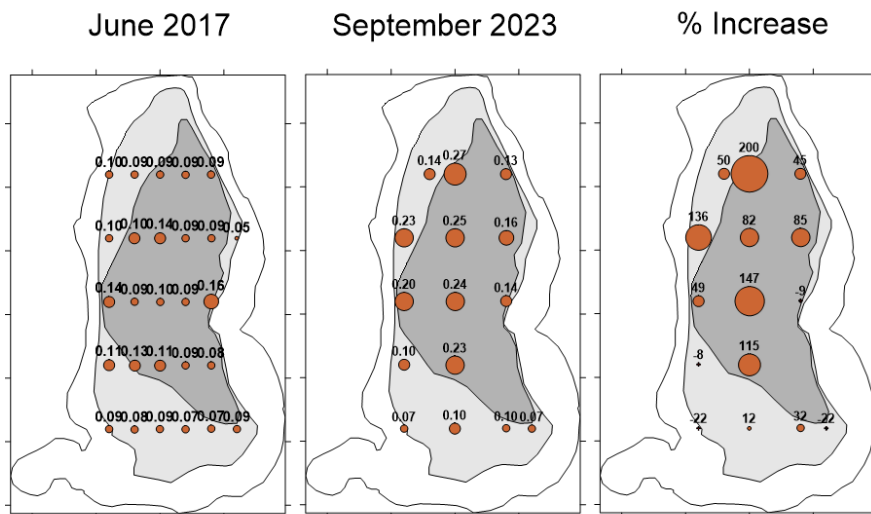
Figure 24. Total aluminum concentrations (mg/g) in the upper 10-cm sediment layer at several stations located at > 25 ft, and a shallower station located between 20 ft and 25 ft. The > 25-ft depth contour was treated with a total of 121 g/m^2 while the 20-25-ft depth contour has been treated with a total of 68 g/m^2 alum since 2017.

Figure 25. A comparison of spatial variations in surface sediment redox P (upper) and aluminum-bound P (lower) immediately before the initial alum treatment in 2017, after the 4th alum application in 2023.

Figure 26. Vertical variations redox P (i.e., the sum of the loosely-bound P and iron-bound P sediment fractions) and aluminum (Al)-bound P concentrations for a sediment core collected from station WQ2 (Figure 1) in June 2017 and September 2023. The sediment profile in June 2017 represents pre-treatment conditions while September 2023 represents post-alum treatment conditions after four alum applications (2017, 2019, 2021, and 2023).
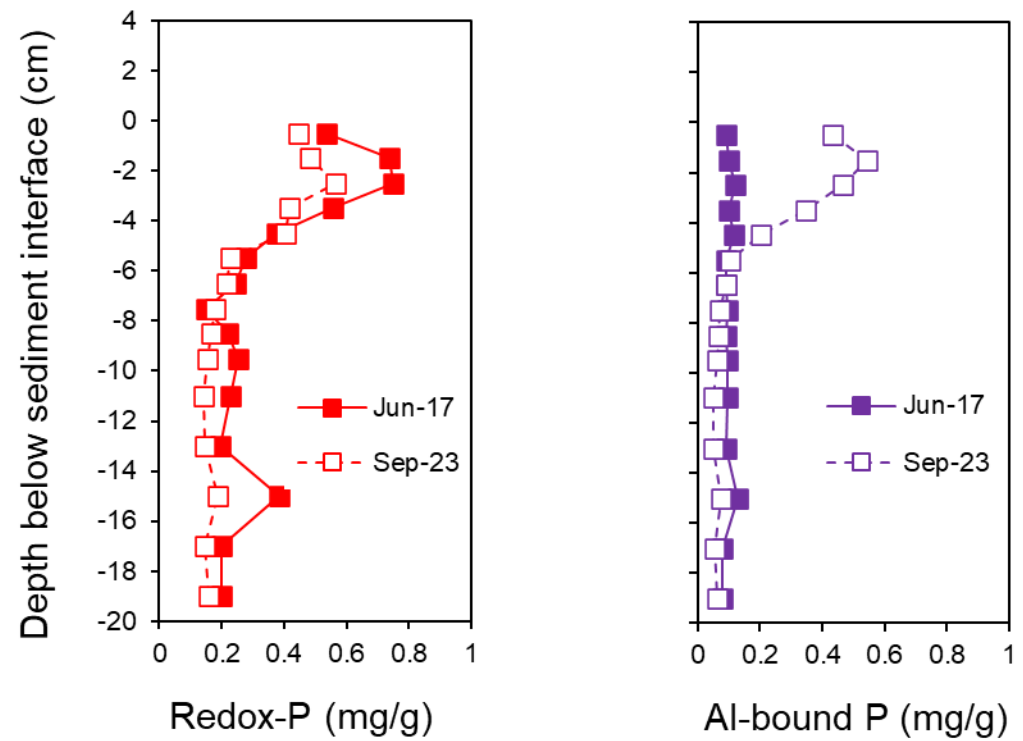
Appendix 1. Detailed vertical water column profiles of water temperature, dissolved oxygen, total P, soluble P, and chlorophyll for various dates in 2023.

Temperature (C)

Dissolved oxygen (mg/L)

Total P (mg/L)

Soluble P (mg/L)

Chlorophyll (ug/L)